

Review

Current Development in Biomaterials—Hydroxyapatite and Bioglass for Applications in Biomedical Field: A Review

Diana Georgiana Filip¹, Vasile-Adrian Surdu^{1,2,*}, Andrei Viorel Paduraru¹ and Ecaterina Andronescu^{1,2,3}

¹ Department of Science and Engineering of Oxide Materials and Nanomaterials, Faculty of Chemical Engineering and Biotechnologies, University Politehnica of Bucharest, 060042 Bucharest, Romania

² National Centre for Micro and Nanomaterials, University Politehnica of Bucharest, 060042 Bucharest, Romania

³ Academy of Romanian Scientists, 50085 Bucharest, Romania

* Correspondence: adrian.surdu@upb.ro

Abstract: Inorganic biomaterials, including different types of metals and ceramics are widely used in various fields due to their biocompatibility, bioactivity, and bioresorbable capacity. In recent years, biomaterials have been used in biomedical and biological applications. Calcium phosphate (*CaPs*) compounds are gaining importance in the field of biomaterials used as a standalone material or in more complex structures, especially for bone substitutes and drug delivery systems. The use of multiple dopants into the structure of *CaPs* compounds can significantly improve their in vivo and in vitro activity. Among the general information included in the Introduction section, in the first section of this review paper, the authors provided a background on the development of hydroxyapatite, methods of synthesis, and its applications. The advantages of using different ions and co-ions for substitution into the hydroxyapatite lattice and their influence on physicochemical, antibacterial, and biological properties of hydroxyapatite are also presented in this section of the review paper. Larry Hench's 45S5 Bioglass[®], commercially named 45S5, was the first bioactive glass that revealed a chemical bond with bone, highlighting the potential of this biomaterial to be widely used in biomedicine for bone regeneration. The second section of this article is focused on the development and current products based on 45S5 Bioglass[®], covering the historical evolution, importance of the sintering method, hybrid bioglass composites, and applications. To overcome the limitations of the original biomaterials, studies were performed to combine hydroxyapatite and 45S5 Bioglass[®] into new composites used for their high bioactivity and improved properties. This particular type of combined hydroxyapatite/bioglass biomaterial is discussed in the last section of this review paper.

Keywords: bioceramics; biomaterials; 45S5 Bioglass[®]; hydroxyapatite



Citation: Filip, D.G.; Surdu, V.-A.; Paduraru, A.V.; Andronescu, E. Current Development in Biomaterials—Hydroxyapatite and Bioglass for Applications in Biomedical Field: A Review. *J. Funct. Biomater.* **2022**, *13*, 248. <https://doi.org/10.3390/jfb13040248>

Academic Editor: Stefano Bellucci

Received: 20 October 2022

Accepted: 14 November 2022

Published: 16 November 2022

Publisher's Note: MDPI stays neutral with regard to jurisdictional claims in published maps and institutional affiliations.



Copyright: © 2022 by the authors. Licensee MDPI, Basel, Switzerland. This article is an open access article distributed under the terms and conditions of the Creative Commons Attribution (CC BY) license (<https://creativecommons.org/licenses/by/4.0/>).

1. Introduction

Even if numerous researchers are actively working to improve bioceramics functions, they have not yet established a definition of bioceramics. According to the Consensus Conference of the European Society of Biomaterial—Chester, England (1986), biomaterials are “any substances, other than a drug, or combination of substances, synthetic or natural in origin, which can be used for any period of time, as a whole or as a part of a system which treats, augments, or replaces any tissue, organ or function of the body”. Taking into consideration this definition, different types of ceramics used in medical and dental fields for the human body are classified as bioceramics. Some opinions are still different for bio-technology-related ceramics, such as immobilized ceramics, carriers of enzyme, and ceramics devices that are used for the separation or purification of proteins [1].

Biomaterials are a perfect alternative for conventional materials used in numerous biomedical applications as they manifest a low or negligible toxicity in relation to humans,

other organisms, and to the environment. Applications of different groups of bioceramics include the replacement, repair, or regeneration of bone or teeth and coating of metallic implants [2–5] but is not limited to this. Hench and Wilson states that biomaterials are bioinert, tolerable, bioactive, and resorbable [6] and due to their interactions with bones or soft tissue, once inside the human body, biomaterials may form direct chemical bonds and accelerate the healing process and/or improve device adherence [7]. Without doubt, the most explored areas of biomaterials research are tissue engineering, drug delivery, and bone regeneration. In Figure 1, a schematic diagram containing various applications of biomaterials is presented [8].

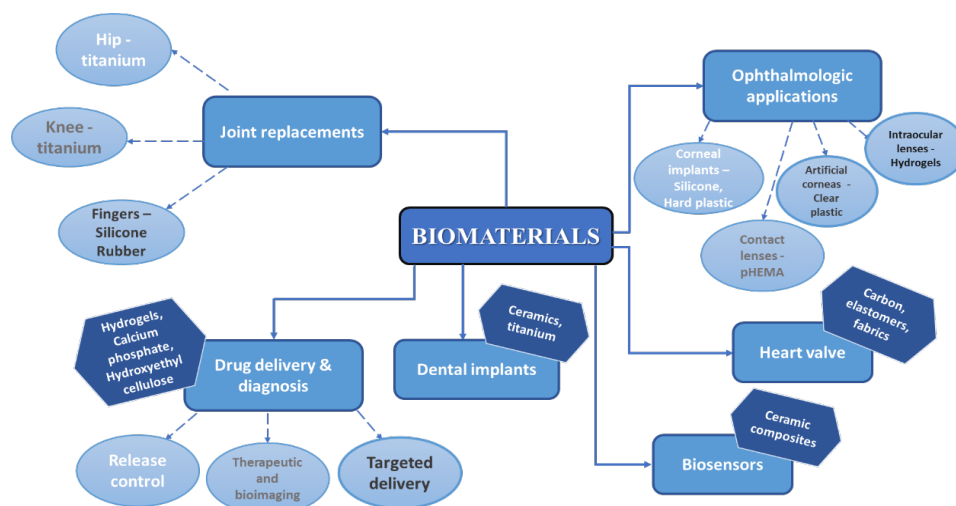


Figure 1. Schematic diagram of different categories of biomaterials and their applications [8].

It is well known that almost 70% of human bone consists in the calcium phosphate (CaP) mineral, and as a consequence, CaP s biomaterials are the first choice for repairing damaged bones. The advantages of CaP biomaterials are the following: low cost, stability, safety, and simple certification for clinical use. Even if the first commercial CaP bone graft substitutes were made available 40 years ago, in the past years a massive development was made to extend the use of CaP in the biomedical field, as carrier for ion delivery, for biologically active agents, and in the field of biomineralization [9]. Recent studies are focused on nearly inert bioceramics and bioactive bioceramics (and biodegradable) [10,11] and bioglass and hydroxyapatite are part of this category [12].

Hydroxyapatite (HAp , molecular formula $Ca_{10}(PO_4)_6(OH)_2$) is the main inorganic constituent of human hard tissues [13] and due to its osteogenic, osteoconductive, and osteoinductive properties, is frequently used as synthetic cement for bone and dental reconstruction [14,15]. The porous surface and biodegradable properties enables HAp to be successfully used in chemotherapy and antibiotic drug delivery systems [16–19].

In 1971, Larry Hench published a peer research paper in which he presented the development of a bone-bonding calcia-phosphosilicate glass–ceramic [20]. This material is now commercially named Bioglass® [21], a particular type of bioactive glass with $Na_2-CaO-SiO_2-P_2O_5$ structure [22]. The evolution of bioactive materials used for implants and repair or replacement of bones is based on the discovery made by Hench. The current global situation has increased public consciousness on the importance of having the best protocols to prevent the spread of microorganisms. The development of novel antimicrobial biomaterial coatings and surfaces has gained attention [23].

In this review paper, the authors summarized recent and relevant studies on hydroxyapatite and Bioglass. According to numerous studies, the substitution of various types of ions into hydroxyapatite and bioglass lattice can increase the performance of the biomaterial and can positively influence the applications, aspects that are furthered investigated in this paper.

2. Focus on Hydroxyapatite

Biomaterials are traditionally used in the medicine field for different types of implants [24–26], but with recent scientific and technological developments, the field of biomaterials has grown, and new improved materials are widely studied for different applications. Calcium phosphates (*CaPs*) are more biocompatible than many other categories of ceramics and inorganic nanoparticles. Due to their biocompatibility and variable stoichiometry, surface charge density, dissolution properties, and functionality, *CaPs* are suitable to be used as drug and growth factor delivery [18]. Hydroxyapatite is also used in multiple non-medical sectors, such as chemical sensors for liquid chromatography column [27], gas sensors, catalysts, [28] or in wastewater treatment [29]. Calcium phosphates exist in different forms, depending on temperature, impurities, and the presence of water molecules [30]. The bioactivity properties and degradation behavior are determined by Ca/P ratio, crystallinity, and phase purity [30–32].

2.1. Structure of Hydroxyapatite

Hydroxyapatite has a complex chemical structure, with Ca/P ratio of 1.67, a hexagonal symmetry S.G. $P6_3/m$ with lattice parameters $a = 0.95$ nm and $c = 0.68$ nm [19,33], and it is the most stable calcium phosphate salt at normal temperatures and pH between 4 and 12 [34]. Ca^{2+} , PO_4^{3-} , and OH^- ions are distributed over 2 symmetric parts of the unit cell and each unit cell of *HAp* contains 10 Ca^{2+} atoms distributed in 2 sites, 6 PO_4^{3-} ions in the tetrahedron, and 2 OH^- ions surrounding the Ca^{2+} ions at the corners of the unit cell (Figure 2). The apatite structure has a carbonate group in two positions: the OH^- sub-lattice generating type A carbonate apatite or the $[PO_4]^{3-}$ sub-lattice generating type B-apatites. When high temperature is used in the synthesis process, type A apatites are obtained [35].

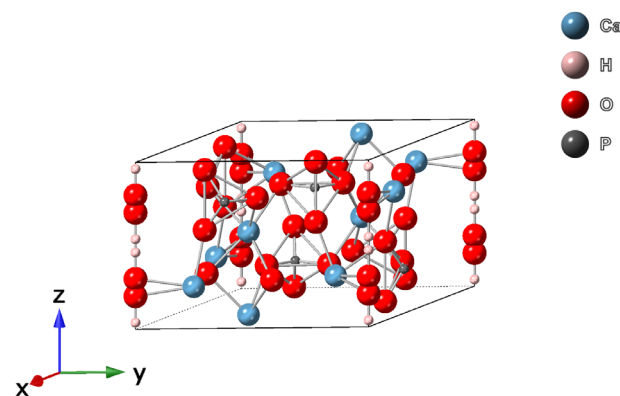


Figure 2. The molecular structure of hydroxyapatite—unit cell perspective of hexagonal crystal structure with $P6_3/m$ symmetry [36,37].

2.2. Synthesis of Hydroxyapatite

Expected performance of the material, economic aspects, precursors, type of solvent used, and the necessary surfactant material, but also the distribution of particles, the need of complex expensive additional steps, and the possibility of agglomerations or impurities in the crystalline structure, are taken into consideration when choosing a synthesis method. Most researchers focused their studies on controlling these parameters by developing new routes of synthesis or by modifying existing routes [38].

HAp can be obtained using a variety of methods, such as sol–gel, chemical precipitation, polyol, hydrothermal, sonochemical and microemulsion, solid-state method, or combustion and thermal decomposition. Recently, due to the attention on environmental issues, innovative methods of synthesis were developed, such as biomimetic methods or the use of hydrothermal molten salt [39]. Depending on the method of synthesis, *HAp* particles can have different sizes and shapes, as presented in Table 1.

Table 1. Comparison between hydroxyapatite nanostructures of different sizes and morphology depending on the synthesis route.

Synthesis Technology	Advantages	Morphology and Size
Co-precipitation [40–43]	The most efficient method at room temperature. The particle size depends on the pH and ionic strength of the reaction media.	Rod, sphere, fiber, tube, filament, whisker, flower Size: 3 nm–1000 µm
Sol-gel method [40,44]	The mixing of reactant at molecular level may improve the chemical homogeneity.	Sphere, needle, tube, rod, filament, platelet Size: 3 nm–1000 µm
Hydrothermal method [40,45–47]	Enhanced solubility of precursors.	Irregular, rod, needle, fiber, whisker, feathery structures Size: 5 nm–8 µm
Sonochemical [40,48–50]	The possibility of producing monodispersed nanoparticles of different shapes.	Sphere, filament, tube, rod Size: 5 nm–1000 µm
Thermal decomposition [40,51–53]	Method that allows a good particle size control and good crystallinity.	Flake, plate, sheet, formless particles Size: 5 nm–200 µm
Combustion [40,54,55]	A quick method with high purity and a single step procedure.	Sphere, oval, irregular spherical shapes Size: 5 nm–200 µm
Solid-state dry synthesis [40,56,57]	Particles with a well-crystallized structure.	Irregular, rod, needle, whisker Size: 5 nm–1000 µm
Biosources [58–61]	Ecofriendly technique to transform waste from various natural sources to wealth.	Different shapes: flakes, plate, rod, tubular shape, etc. Size: 10 nm–2000 µm

The possibilities of synthesis *HAp* can be classified as:

- Wet-chemical synthesis: precipitation, hydrothermal, and sol-gel method;
- Dry-chemical synthesis: solid-state reactions and mechanochemical method;
- High-temperature methods: combustion, spray pyrolysis, and thermal decomposition;
- Use of bioresources: animal sources (sheep, pig, and goat teeth and bones); marine sources (bones, red algae, fish scale, corals, or seashells); and plant sources (bamboo, potato orange banana peels, calendula flowers, etc.).

2.3. Substitution of Various Ions in *HAp*

HAp has an excellent biocompatibility, but the bioactivity can be enhanced using substitution ions in its unit cell [62]. One disadvantage of synthetic stoichiometric *HAp* is having poor mechanical properties, and thus is not indicated to be used as a standalone material [63]. *HAp* is able to accept various compositional structures in its sub-lattices, and depending on which substitution ions are used, a new *HAp* composite with improved properties for specific biomedical applications can be obtained [64,65]. If we consider the evolution of trends in the type, frequency, and competition of dopants used, it can be observed that 72 elements of the periodic table were successfully incorporated into its structure. The overall use of individual chemical elements as dopants in *HAp* is presented in Figure 3 [66]. Chemical elements are marked with different colors, depending on the number of studies that were published with doped hydroxyapatite. The number of studies can be found in the legend.

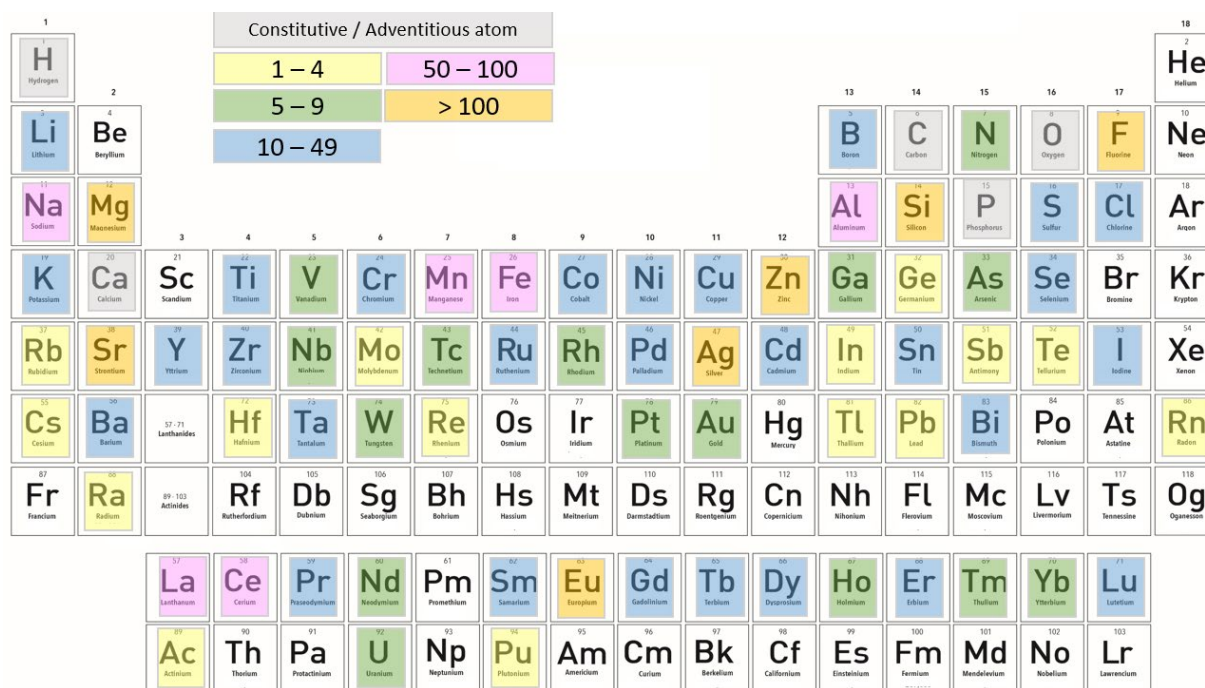


Figure 3. Periodic table of elements—each element has a corresponding color (yellow, green, blue, pink, and orange) which suggests the total number of its literature reports. The only adventitious element is carbon because most HAp crystals precipitated under the atmospheric conditions contain finite amounts of the carbonate ion. For this statistic, Scopus and Google Scholar search engines were used [66].

With a flexible hexagonal structure, HAp can be substituted with numerous cationic ions (Sr^{2+} , Na^+ , K^+ , Mg^{2+} , Zn^{2+} , Ag^+ , etc.) and anionic ions (CO_3^{2-} , SiO_4^{4-} , SeO_3^{2-} , F^- , Cl^- , Br^- , and others) [67]. The shorter distance from Ca II sites and the Ca II-O bond makes cations with smaller size than Ca atoms to be preferred for substitution [68,69]. It has been proven that after substitution, HAp will have the same hexagonal structure, but the minor internal tensions can cause changes in thermal stability, solubility and hardness. The use of various doping ions that enter into the structure of hydroxyapatite can enhance mechanical performance and also improve multiple biofunctionalities, such as osteogenesis, resistance to adhesion, and proliferation of bacterial strains [70].

2.3.1. Cationic Substitutions

Cationic substitutions are performed by replacing Ca^{2+} ions from hydroxyapatite's lattice with monovalent ions (lithium—Li [71], sodium—Na [72], silver—Ag [73,74]), bivalent ions (magnesium—Mg [75], strontium—Sr [76], zinc—Zn [77]) or multivalent ions (aluminum—Al [78], cerium—Ce [79], gallium—Ga, or titanium—Ti [80]). The cationic substitution has been extensively studied, but it has been shown that not all the elements can be used for improved biofunctional properties. The advantages of using Zn, Mg, and Sr is that these ions have the capability to increase the osteogenic capacity. Co has angiogenic activity, and the use of Ce, Zn, and Ag cations for substitution offers excellent antimicrobial properties.

Multiple ions can be used for cationic substitution. From all the elements, Magnesium is one of the key elements because human bones contain about 60% of Mg^{2+} so it has an essential role in the health of teeth and bones. Magnesium ions have the potential to influence bone metabolism, cell adhesion and proliferation, and a deficiency in Mg^{2+} can cause bone fragility, stoppage of bone growth, and osteopenia [81,82]. Mg-doped hydroxyapatite can be synthesized by an aqueous precipitation method [83,84], but the use of hydrothermal technology was also reported [85]. As published by Matsunaga [69], the

formation energies of smaller ions in hydroxyapatite structure decreases with the increase in pH of the solution. Ca^{2+} are released from the hydroxyapatite lattice at lower values of pH, and the effect is in reverse with the increase in pH values. If smaller size cations are replacing the Ca^{2+} atoms, the adjacent O^{2-} atoms tend to move to substitute cations because of the difference in ion size. Once the Ca^{2+} ions are substituted by Mg^{2+} ions, the unit cell volume will decrease and the result is a smaller ionic radius of 0.072 nm. Various secondary products are formed with the synthesis of Mg-doped hydroxyapatite, such as $\text{Mg}(\text{OH})_2$, brushite at higher degrees, or β -tricalcium phosphate [86]. The formation of CaP as secondary products is the result of the limited degree of substitution of magnesium ions in hydroxyapatite structure. Besides the beneficial effects of substitution of Mg in the HAp lattice related to bone structure, antibacterial properties against *E. coli*, *P. aeruginosa*, *S. aureus*, and *C. albicans* were also demonstrated [75,87].

Due to their smaller radius of 0.074 nm, Zn^{2+} ions are theoretically more appropriate to be used for the substitution of hydroxyapatite. Zn-doped hydroxyapatite is suitable to be used in biomedical field due to the effects of Zn^{2+} on metabolic processes. Generally, a precipitation method at room temperature [88] or at 60–90 °C [89] is used, but there are also studies which reported the use of other technologies, such as ion exchange, hydrothermal synthesis, and the sol–gel method [90]. The crystallinity of hydroxyapatite is reduced when substitutional ions with smaller size are used. The explanation may be that the ions are partially incorporated, leading to the inhibition of crystal growth. The antibacterial properties of Zn-doped hydroxyapatite increase with the increase in Zn^{2+} ions content. Zn/HAp biomaterial can be used on stem cell differentiation and because of the antibacterial properties, the biomaterial might be used as a coating on metal implants [91].

Some studies have demonstrated that $\text{Fe}^{2+}/\text{Fe}^{3+}$ ions can improve tissue regeneration, but the deficiency of Fe ions could contribute to the inhibition of osteoblast cell mineralization [92]. Fe^{3+} substitution in HAp structure leads to a decrease in particle size and an increase in hardness and dielectric properties for HAp . Similarly, this biomaterial is suitable for drug release systems, is blood-compatible in nature, and has an increased bioactivity. Fe-doped hydroxyapatite is obtained using precipitation, hydrothermal, and reflux methods, without the formation of other crystalline phases. Antibacterial tests suggest that Fe-substituted HAp is strongly active against bacterial strains and can be used for antibacterial applications [93].

It is well known that lanthanides have high bioactivity and the ability to substitute calcium ions in molecules due to their narrow emission bands and long emission lifetime. Lanthanides are widely used for magnetic resonance imaging and as luminescent probes for biosensors for in vivo imaging applications [94]. Even if they are less studied than other chemical elements, Cerium ions possesses excellent antioxidant properties against oxidative stress-induced cell damage and Ce-doped HAp nanomaterials have no cytotoxic effect. Therefore, the Ce-doped nanomaterials could be used for cellular imaging [95]. Due to its two forms, Ce^{3+} and Ce^{4+} have the unique property to switch between oxidation states and recent studies have shown that the reduction of CeO_2 from Ce^{4+} to Ce^{3+} happens due to the formation of oxygen vacancies without changing its own structure [96]. Among the numerous techniques for preparation of Ce-doped hydroxyapatite, researchers mostly used the co-precipitation method [79], hydrothermal technique [97], sol–gel method [98], microwave irradiation technique [99], and ultrasonic-assisted precipitation synthesis [98]. Sol–gel preparation is the preferred method due to its simplicity, reduced additional costs, ease of handling, requirement of lower temperature, and the high purity and crystallinity of Ce-doped HAp particles [100,101].

2.3.2. Anionic Substitutions

In contrast with monovalent anions (F^- or Cl^-) that can substitute OH^- groups, bivalent anions (HPO_4^{2-} , SO_4^{2-} , SeO_3^{2-} , CO_3^{2-}) are able to substitute PO_4^{3-} groups with formation of hydroxide and calcium vacancies. As already evidenced in several studies, carbonate ions are naturally present in biological apatite structure in 4–8 wt.% [102]. The

CO_3^{2-} group can partially replace both PO_4^{3-} groups in the B sites of the hydroxyapatite structure, leading to B-type substitution, or the hydroxyl ion, leading to A-type substitution. The B-type substitution is found in the bones of most species, where the A/B ratio is in the range 0.7–0.9. For A-type substitution, the experimental procedure should be performed at a temperature of 800 °C–1000 °C in a dry CO_2 atmosphere. B-type substitution is mostly obtained by wet precipitation under atmospheric conditions. A combined A/B-type substitution was also identified when two CO_3^{2-} ions replace one hydroxyl group and one phosphate group. As a source of carbonate ions, sodium hydrogen carbonate (NaHCO_3) [103,104], di-ammonium carbonate ($(\text{NH}_4)_2\text{CO}_3$) [105], or calcium carbonate (CaCO_3) can be used [106]. The substitution can be carried out by multiple routes, such as wet chemical precipitation, emulsion methods, co-precipitation, mechanochemical methods, sol-gel synthesis, or microwave precipitation [107]. Carbonate-substituted hydroxyapatite can potentially be used in bone regeneration due to its effect on cell proliferation compared with stoichiometric *HAp* and the effect of the synthesized material depends on the percentage of CO_3^{2-} substitution [108,109]. In some in vitro studies, it was reported that the production of collagen by human osteoblast cells was increased by carbonated hydroxyapatite, compared with pure hydroxyapatite. This is related to the production of type I collagen, higher in cell culture medium with carbonated hydroxyapatite, depending on extracellular calcium concentration [110].

2.3.3. Effects of Co-Doping on Physicochemical, Antibacterial, and Biological Properties of *HAp*

Co-doped hydroxyapatite can be synthesized from synthetic precursors and/or from biogenic sources. Ag^+ , Zn^+ , Cu^{2+} , and F^- act as antibacterial agents; M^{82+} , Sr^{2+} , and Mn^{2+} improve bone metabolism; and SeO_3^{2-} , SeO_4^{2-} , and Fe^{3+} have anti-cancer properties. The type, size, and concentration of ionic substitution agents can lead to changes in the microstructure, grain size, thermal stability, lattice parameters, crystal morphology, crystallinity, and solubility of *HAp*.

The substitution of Zn^+/Cl^- ions in the *HAp* lattice using the precipitation method increased the degree of crystallinity in comparison with pure *HAp*. It was demonstrated that Zn atoms occupy the interstitial sites in hydroxyapatite and does not substitute Ca atoms in Ca(I) or Ca(II) sites. Slight changes in unit-cell volume were noted when the Zn^{2+} cation is placed in site 2*b* in *HAp*, due to the increase in the *c* lattice parameter and the decrease in the *a* lattice parameter [111,112].

For Y^{3+} and F^- ions that have a smaller ionic radius size compared with Ca^{2+} and OH^- , studies revealed that after substitution, the lattice parameters and unit cell volume of *HAp* decreased [113,114]. According to another study, the use of a high concentration of 7.5 mol% Y^{3+} and 2.5 mol% F^- caused a decrease in relative density, but if the synthesis was performed at a temperature higher than 1300 °C, the relative density increased [115]. The samples analyzed by Raman spectroscopy confirmed that Y^{3+} and F^- ions used as co-doping agents for *HAp* led to perturbation in the hexagonal structure, shifting Raman bands to further bands located inside the spectra of Y/F-*HAp* [116].

The effect of use of Al^{3+} and F^- ions as co-substitution agents for hydroxyapatite was also studied. The samples were obtained by the precipitation method and sintered at 1100 °C. The increase in sintering time and concentration of co-doping ions led to an increased density in Al/F-*HAp* and a decrease in lattice parameters. Generally, the presence of Al^{3+} ions may have a negative effect on mechanical properties of the biomaterial and, therefore, Mg^{2+} ions are preferred instead [117].

Another study was focused on the effects of Mg^{2+} and various amounts of Ni^{2+} ions for co-doping. The samples were synthesized at 870 °C by wet chemical method and the concentration of Ni^{2+} ions was 0%, 0.6%, 1.2%, and 1.8 % at. The Ni^{2+} concentration influenced the lattice parameters and crystallinity degree, as well as the unit cell volume [118].

Using the microwave refluxing system, substitution of *HAp* with Fe^{3+} and selenite (SeO_4^{2-}) ions was also studied. Micrograph images of *Fe/Se-HAp* samples showed that the morphology was influenced by the increase in Fe^{3+} concentration [119].

Depending on the properties that are expected on the material, a combination of doping agents can be used. In Figure 4, the synthesis technology for ionic-substituted *HAp* and the effects of ions for different properties of material is presented [120]. The combined effect of the doping ions can be modified depending on the synthesis method preferred in order to obtain the desired dissolution rate of the biomaterial. The effects of co-doping on biological performance are summarized in Table 2. Sr^{2+} ions are usually used for doping hydroxyapatite to intensify osteogenesis and offset the negative effect of other ions. Bismuth is also considered to be a proper substituent for *HAp* and the co-substituted *Sr/Bi-HAp* biomaterial has high antibacterial activity against *E. coli* [121]. $\text{Cu}^{2+}/\text{HAp}$ samples show high antibacterial activity, but the synthesis should be performed carefully because Cu^{2+} could be toxic to human cells at high concentrations [122]. Zn^{2+} has an important role in the osteogenesis process in bone remodeling. Published studies demonstrated that the toxicity level of Zn^{2+} ions was increased up to 6 wt.% and the samples showed antibacterial properties against *E. coli* and *S. aureus*.

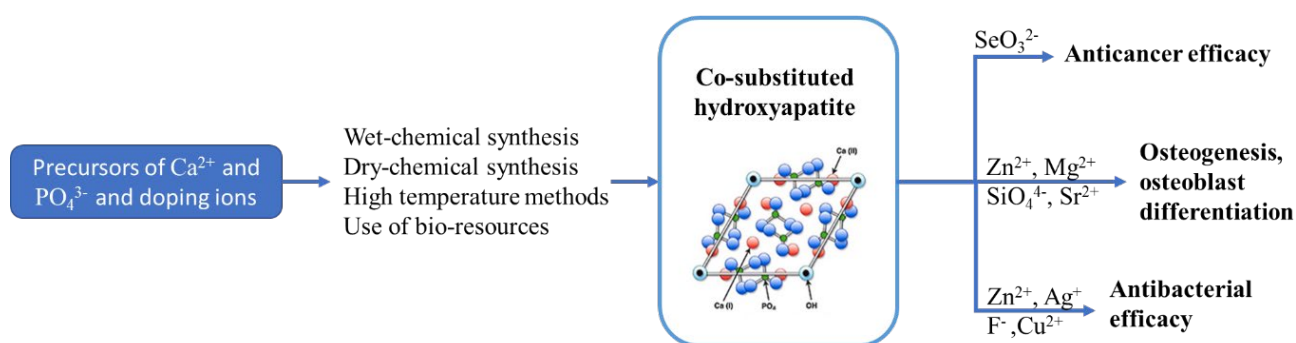


Figure 4. Schematic representation of synthesis methods for doped hydroxyapatite and the effect of the doping ions on anticancer, antibacterial, and osteogenesis properties [90].

Along with Zn^{2+} and Cu^{2+} , studies were performed to demonstrate that Ag^+ ions have excellent antibacterial activity. Ag^+ ions are frequently used as a dopant agent for hydroxyapatite for antibacterial applications due to its large spectrum of antimicrobial activity. The most common use is in the medical field for vascular grafts and implants because of its antiseptic properties for wound dressing and burn creams [123]. Ag^+ ions are widely used for antimicrobial biomaterial applications as they can influence the bacterial replication process and possible cell death [124,125].

In a similar way, Ti^{4+} was also incorporated into the structure of *HAp*, together with Zn^{2+} , Ag^+ , and Cu^{2+} ions using the co-precipitation method. The results were excellent for *Ti/Ag-HAp* and *Ti/Cu-HAp* which exhibit a high efficiency against *E. coli* and *S. aureus* under weak UVA irradiation due to the combination of oxidation character of O_2^- radicals and antibacterial properties [126].

Numerous types of ions are used as substitution agents for hydroxyapatite and various studies are available to gain more knowledge on this field. On the other hand, depending on the expected properties of the synthesized biomaterial and the applications, researchers can modify the dopant, the synthesis conditions, and can choose the appropriate technique. A good progress was made through the years to obtain novel biomaterials with sustainable long-term antimicrobial properties, but the use in clinical applications is still in development stage. The use of hydroxyapatite in various combinations with other types of biomaterials in order to improve and widen biomaterial applications is further studied in this paper.

Table 2. Biological performance of various co-doping agents.

Co-Doping Agents	Synthesis Method	Biological Performance
Zn ²⁺ , SeO ₃ ²⁻ [120]	Precipitation method	Cytotoxic for BALB/c 3T3 mouse fibroblasts
Zn ²⁺ , Cu ²⁺ [122]	Electrolytic deposition	Antibacterial properties, promoting the MC3T3-E1 osteoblasts cell viability
Zn ²⁺ , Sr ²⁺ [127]	Hydrothermal method	Antibacterial properties, improving the cytotoxic limit of Zn ²⁺ , adhesion
Sr ²⁺ , Ag ⁺ [124]	Hydrothermal method	Antibacterial properties, high osteoinductive properties, promote ALP activity in vitro
Sr ²⁺ , Bi ³⁺ [121]	Microwave-assisted precipitation method	Antibacterial properties
Sr ²⁺ , F ⁻ [121]	Hydrothermal method	Antibacterial properties, promote ALP activity
SiO ₄ ⁴⁻ , Ag ⁺ [128]	Precipitation method	Enhanced osteoconductive properties in vitro
Sr ²⁺ , Ag ⁺ , F ⁻ [125]	Electrolytic deposition	Induce bone formation, high early bone integration ability

3. Focus on Bioactive Glasses, Bioglass[®] 45S5

All bioactive materials have the capability to form an interfacial bond with bones or tissues, but the type of biomaterial influences the time dependence of bonding and the strength, thickness, and mechanism of bonding. Bioactive glasses have higher potential to stimulate bone regeneration compared with other types of bioactive ceramics.

3.1. Structure and Synthesis of Bioglass

Silica-based bioactive glasses are a group of surface-reactive glass–ceramic biomaterials. Hench et al. [20] were the first to obtain the first-generation bioglass at the University of Florida. The compound known as Bioglass[®] (commercial name: 45S5 BG) is a quaternary system, composed of 45% silica (SiO₂), 24.5% sodium oxide (Na₂O), 24.4% calcium oxide (CaO), and 6% phosphorus pentoxide (P₂O₅) as weight percent, the last component being added to simulate the Ca/P ratio of hydroxyapatite [129]. The name 45S5 comes from the weight percent of silica as the network former and the 5 to 1 molar ratio of Ca to P. The paper published in 1971 by Hench presents the composition of the Bioglass and the results obtained by transmission electron microscopy (TEM), confirming the bonding to bone. Additionally, other research was conducted to test substitution of SiO₂ with B₂O₃ (5–15 wt.%) and the substitution of CaO with CaF₂ (in a concentration of 12.5 wt.%), but the substitutions did not improve the capacity of the material to form a bone bond [6]. In Table 3, the most important steps for the development of bioactive glasses and timeline are presented.

Table 3. Development of 45S5 Bioglass®.

Year	Development Steps
1969	45S5 Bioglass® was discovered at the University of Florida
1971	Based on the research activity, bonding of bone to bioactive glasses and glass–ceramics study was published [20,130]
1975	Bioglass-coated alumina was used for bone bonding on sheep hip implants [131]
1977	Bioglass coating on metals and alumina ceramics was patented [132]
1981	Discovery of soft connective tissue bonding to 45S5 Bioglass® [133]
1988	Bioglass is approved by FDA to be used on ERMI implant [132,134,135]
1991	Sol–gel synthesis was investigated for bioactive gel-glasses [136,137]
1993	PerioGlas® was approved by FDA to be used for bone and dental repair [138]
1996	PerioGlas® (bioglass used for bone grafting) is used in tooth extraction and alveolar augmentation [132]
1999	TheraSphere® was approved by FDA to be used for cancer treatment [138]
2000	Studies were made to examine if 45S5 Bioglass® can be used to control osteoblast cell cycles [139]
2004–2005	NovaMin® (particular type of 45S5 Bioglass®) is developed for use as repair agent in toothpaste [132]
2010	Cardiac tissue engineering [138]
2012	Spinal cord repair [138]
2018	TheraSphere® is used for liver metastatic colorectal carcinoma [138]

Originally, 45S5 Bioglass® was produced by melt-processing of oxides with high-purity in a furnace at 1370 °C. The melt mixture is poured into water to quench, obtaining a frit. Next steps are drying and grinding, in order to obtain the appropriate particle size range. The Bioglass can be transferred into molds and rods or as-cast components can be produced [140]. This method is considered simple and suitable for higher quantities of products. However, the shortcoming of the method is the evaporation of P₂O₅ because of the high temperatures involved. Recent studies were focused on the sol–gel technique. This method requires a lower temperature than the traditional technique and gives the possibility to obtain a homogeneous composition [141]. Additionally, if clinical applications are considered, a method that will avoid contamination of the final product is preferred. The traditional crucible method can be replaced with a containerless technique, which allows fine control of the bioglass purity. The advantages of using the containerless technique instead of the traditional method, where the interactions of the prepared samples with the crucible wall create internal stress, are the achievement of supercooled liquids, rapid solidification, and suppression of heterogeneous nucleation [142].

3.2. Clinical Applications of 45S5 Bioglass® and Bioceramics

Bioactive materials promote an adherent interface with tissues, sufficient to resist mechanical fracture. With excellent biocompatibility, stimulatory effects on bone cell functions and the capacity to link with bone via chemical bond and with other tissues, bioactive glass is currently used for applications in orthopedic and dental fields, to replace bones or teeth, dental devices, or as a coating for orthopedic anchors [143]. The bioactivity of Bioglass® is based on its amorphous structure, but depending on the composition, the bioactivity, bioresorbability, and osteoconductivity could be modified [144]. In Table 4, the key roles of Bioglass in medical and dental fields are listed [132]. A novel discovery in

this area is the use of Bioglass in preventive treatments—for prevention of dentinal pain sensitivity and for its effects on inhibition of gingivitis.

Table 4. Orthopedics, cranial–facial and dental–maxillofacial products based on 45S5 Bioglass® [132].

Medical Field	Applications
Orthopedics products	Trauma:
	Fractures of long bones (alone or with internal fixation)
	Repair of femoral
	Tibial plateau fracture
	Arthroplasty:
	Filler around implants
Cranial–facial products	Impaction bone grafting
	Spine fusion:
	Posterolateral lumbar spinal fusion
	Recovery of bones after tumor removal
	Cranioplasty:
Dental–maxillofacial products	Facial reconstruction
	Augmentation of alveolar ridge
	General dental/oral improvement:
	Sinus lift surgery
	Cutting or reshaping of bones
	Repair of periodontal defects
	Toothpaste and treatments to prevent hypersensitivity
	Obliteration of frontal sinus
	Direct and indirect pulp capping
	Repair of orbital floor fracture

In 1985, FDA approved the first medical device based on 45S5 Bioglass®, commercialized under the name “Bioglass® Ossicular Reconstruction Prosthesis” or “Middle Ear Prosthesis” MEP®, a medical device used to treat conductive hearing losses. Another medical device called Bioglass®-EPI was developed 30 years ago and it was used as an extracochlear percutaneous implant to the temporal bone of patients with hearing loss. Following MEP® and Bioglass®-EPI, another bioglass-based device was commercialized under the name ERMI® in 1988. The Endosseous Ridge Maintenance Implant is used in periodontal surgery [138]. In Finland, researchers developed another material starting from the composition of 45S5 Bioglass®, BonAlive®, used in the orthopedic field as a bone graft substitute. PerioGlas®, a particulate 45S5 Bioglass® product, is now sold by NovaBone Products LLC, Florida, in more than 35 countries worldwide. With a particle size range of 90–710 µm, PerioGlas® is used to regenerate bone teeth for dental intraosseous, oral, and cranio-/maxillofacial bony defects and is also used in combination with polymeric membranes. Biogran®, sold by BIOMET 3i, Florida, has the same composition as 45S5 Bioglass®, the only difference is the particle size of 300–360 µm. This material is a synthetic bone graft used for its bone regeneration effects. NovaBone® (sold by NovaBone Products LLC, Alachua, FL, USA) is used since 1999 to repair bone defects in maxillofacial or orthopedic non-load-bearing sites.

Apart from the commercial forms used to repair bone and teeth defects, other types of 45S5 Bioglass® were developed for oral care. NovaMin®, a specific kind of 45S5 Bioglass®, has a particle size of 18 µm and is used in toothpaste to prevent tooth hypersensitivity and for whitening treatments of teeth [145]. In Table 5, the commercial products mentioned above and their structural differences are presented.

Since 2009, endodontic biomaterials with excellent biocompatibility in vitro and low cytotoxicity, such as Biodentine, ProRoot Mineral Trioxide Aggregate (MTA), and Pulp-Guard, were developed and became commercially available. Several studies revealed that this new type of bioceramics composite biomaterials can enhance cell attachment

and proliferation. These biomaterials are used for direct pulp capping, pulpotomy, or apexification [146,147].

Table 5. Schematic presentation of commercial products based on 45S5 Bioglass®.

Material	Composition and Structure	References
PerioGlas®	Contains calcium, sodium, phosphate and silica; it is a granulated form of 45S5 Bioglass® Particle size: 90–710 µm	[148]
Biogran®	Same composition as 45S5 Bioglass® (calcium, sodium, phosphate, and silica); particles of narrow size range Particle size: 300–360 µm	[149]
BonAlive®	Special bioglass (S53P4), consists of 53% SiO ₂ , 23% Na ₂ O, 20% CaO, and 4% P ₂ O ₅ as weight percent Particle size: 500–800 µm	[150,151]
NovaMin®	Identical with 45S5 Bioglass®, contains only calcium, sodium, phosphate, and silica in an amorphous matrix Particle size: 18 µm	[152]

3.3. Derived Bioglass Bioactive Materials

Even if 45S5 Bioglass® is by far one of the most investigated materials for its capability to repair damaged bone tissues, the clinical cases are vast and may differ, each one being also influenced by human metabolism, patient's age, the severity of the injury, etc. [153]. Significant work was carried out during past years to discover which is the optimum composition of a bioglass and it has been demonstrated that the amount of SiO₂ and Ca/P ratio can be changed in order to improve bioactivity. Researchers developed methods of incorporating various ions such as magnesium (Mg²⁺), calcium (Ca²⁺), cerium (Ce³⁺), zinc (Zn²⁺), aluminum (Al³⁺), and strontium (Sr²⁺) in order to improve bioglass characteristics. Recent studies revealed that bismuth cations (Bi³⁺) are also efficient when incorporated into bioglass lattice, with nanocomposites of bismuth-doped bioglass/graphene oxide being successfully used in bone tissue engineering [154].

It is already noted that strontium can be a substitute for calcium in bioglass structures, with the capability to improve osteoblast activity and to minimize bone fracture [155]. The bioactive coating may impart an antibacterial effect to the environment, not only between bone and implant. Studies have revealed that a small concentration of Sr²⁺ (2.5 mol%) manifests antibacterial properties against *S. aureus*, *E. coli*, and *P. gingivalis*. Ca²⁺ and Sr²⁺ have similar ionic structures, hence the incorporation of strontium ions would modify the dissolution of the bioglasses. The addition of Ca²⁺ in a high amount can lead to a decrease in osteoblast viability. Studies in vitro and in vivo revealed that Sr²⁺ positively influenced osteoblast proliferation and bone formation [156].

Zinc was also added into the bioglass structure due to its beneficial properties on bone formation in vitro and in vivo [157–159]. Raman spectra, EDX microscopy, and studies performed on cell culture revealed that the incorporation of Zn²⁺ into the bioglass system is beneficial for cell attachment. SiO₂-CaO-P₂O₅-ZnO biomaterial is highly bioactive and biocompatible in vitro, and the substitution of Zn²⁺ enhances early cell proliferation and promotes differentiation [129].

Another possibility for substitution is the incorporation of Al³⁺/Sr²⁺ ions in the same amount (2 mol%). Tests revealed that the bioactivity was maintained, even if the alumina influenced the degradation of bioglass. No changes in the bioglass lattice were reported. Moreover, the studied samples exhibited an antibacterial effect against *E. coli* strains. The combined effect of antibacterial activity and biocompatibility promotes bioactive glasses to be used for bone regeneration [157].

The addition of iron oxide (Fe₂O₃) into the bioglass structure reveals the possibility to use the material for magnetic induction hyperthermia treatment of cancer. Specific types of bioglasses (SiO₂-CaO-Fe₂O₃, SiO₂-CaO-Fe₂O₃-B₂O₃-P₂O₅, and SiO₂-Al₂O₃-Fe₂O₃-P₂O₅-

Li_2O) were synthesized by controlled crystallization. Depending on the amount of iron oxide from the samples, studies were made to analyze the evolution of magnetic properties and the crystallite size [160].

Recent development was made for incorporating luminescent materials into the bioglass structure in order to obtain nanoparticles that can be used for biological labelling applications and drug delivery systems [161,162]. The possibility to have luminescence characteristics would be helpful for understanding bioglass degradation in vitro. Er^{3+} and Yb^{3+} were used as co-doping agents for bioglass using a containerless method in an aerodynamic levitation furnace. The tests performed on the $\text{Er}^{3+}/\text{Yb}^{3+}$ co-doped bioglass samples exhibit visible up-conversion luminescence and the cell proliferation assay suggests the biocompatibility and bioactivity of the material for cell proliferation, similar with the pure bioglass [163].

The substitution with other rare earth elements, $\text{Tb}^{3+}/\text{Yb}^{3+}$, into the bioglass structure was studied to obtain a multicomponent bioglass with luminescent properties. The elemental composition of 45S5 Bioglass[®] was standard and the amount of SiO_2 was increased to 50 wt.%, with the Ca/P ratio being maintained at 4:1 as in 45S5 Bioglass[®] and then modified at 1.67. The most important factors for network connectivity and structural properties of bioglass are concentration, the method of synthesis, and temperature. The amorphous nature of bioglass until 700 °C was confirmed by XRD analysis and the in vitro bioactivity test confirmed that all samples of $\text{Tb}^{3+}/\text{Yb}^{3+}$ co-doped bioglass exhibit good apatite-forming ability [164].

4. Hydroxyapatite/Bioglass 45S5 Composites

In order to develop a new hydroxyapatite/bioglass composite, researchers should have the proper information regarding the structure, properties, and applications of the starting biomaterials. This information is summarized in Table 6 [165,166]. Bioactive glass manifests advanced properties in comparison with hydroxyapatite. On a study conducted on rabbits, researchers reported that granules of 45S5 Bioglass[®] can promote bone proliferation more easily than *HAp*, with 45S5 Bioglass[®] being considered osteoinductive due to its capability to support bone growth together or away from the bone–implant interface [167].

Composites containing bioactive glass/hydroxyapatite are extensively studied due to their applications for regeneration and repair of bone tissue. Some studies were focused on the possibility to use bioglass/hydroxyapatite (*BG/HAp*) composite as a coating on titanium substrate. Samples were prepared via the electrophoretic deposition method (EPD), a simple, versatile technique with good cost-effectiveness. The EPD method is based on the movement of charged particles toward the working electrode by applying an electric field [168]. According to Khanmohammadi et al. [169], the combination of 50% *BG*/50% *HAp* exhibits high bioactivity and maximum bonding strength, which will shorten the bioactive fixation of the implant in medical use. The tests performed on the samples shows that the pure bioglass exhibits the lowest bonding strength in comparison with the samples where *HAp* was added.

Another study reported the synthesis of bioglass by the sol–gel method, followed by the synthesis of bioglass/hydroxyapatite biomaterial through a traditional technique, heated in a furnace up to 1000 °C. Different concentrations of hydroxyapatite were used. The bioactivity of *BG/HAp* material was determined by in vitro tests. The synthesized biomaterial exhibits high bioactivity property demonstrated by FTIR and SEM analysis [170].

Rizwan et al. [171] reported the use of Spark plasma sintering method (SPS) to obtain *HAp/BG* composite scaffold materials. SPS technique is a non-conventional method used to obtain composites at low values of pressure and temperature in a short period of time at 1000 °C temperature. The benefits of the method are the easiness of controlling parameters, possibility to obtain amorphous or nanocrystalline phases and to avoid thermal decomposition. The content of hydroxyapatite was in the range of 0–30 wt.%. After the evaluation of prepared samples, it was demonstrated that the SPS sintering method can be used for the *HAp/BG* composite, showing no drastic reactions between components.

Table 6. Presentation of general information about hydroxyapatite and 45S5 Bioglass® [165,166].

Information about Material	Material		
	Hydroxyapatite	45S5 Bioglass®	
Composition	Ca ₁₀ (PO ₄) ₆ (OH) ₂	45 wt.% SiO ₂ , 6 wt.% P ₂ O ₅ , 24.5 wt.% CaO, and 24.5 wt.% Na ₂ O	
Structure	Crystalline, hexagonal symmetry	Amorphous	
Average particle size	10 nm and 500 nm	Commercial products have different particle size, from 18 µm to 800 µm	
Molar mass (g/mol)	502.31	-	
Density (g/cm ³)	3.16	2.7	
Melting point (°C)	1614	Approximately 1100–1200 [172]	
Solubility in water	Poorly soluble in water	More soluble than other bioactive materials such as HAp	
Mechanical properties	Compression strength (MPa)	>400	Approximately 500
	Tensile strength (MPa)	Approximately 40	42
	Elastic modulus (GPa)	Approximately 100	35
	Fracture toughness (MPa√m)	Approximately 1.0	0.5 to 1
Uses and advantages	Desirable bone replacement material due to high hardness and high bioactivity, which accelerate early stage of bone growth	Repair of bone injuries or defects due to high biocompatibility, bioactivity, and osteoconductivity Applications in tissue engineering and tooth enamel reconstruction with high antibacterial resistance	
Antibacterial effect	Low antibacterial properties, doping bacteriostatic ions such as Sr, Zn, Ce, and Ag are used for substitution	Effective against a wide selection of aerobic and anaerobic bacteria [173]	

After analyzing the existing literature and current research we can conclude that the hydroxyapatite/bioglass composite biomaterials have the advantages of both components. Pure bioglass and pure hydroxyapatite show minimum bonding strength, while the HAp/BG composite shows increased bonding strength at 50 wt.% of components. Even if HAp has excellent biocompatibility, the bioactivity is improved for composites with bioactive glass, when a silicate hydroxyapatite may be produced. Hydroxyapatite shows low antibacterial property which leads to investigations focused on modifying doping bacteriostatic ions. Studies demonstrated that 45S5 Bioglass® is efficient against *S. aureus*, *S. epidermidis*, and *E. coli*. The combination of hydroxyapatite and bioglass particles confers special characteristics such as antibacterial effect, bioactivity, and mechanical properties.

5. Conclusions and Future Perspectives

Since calcium phosphates were proposed for the first time to be used in the biomedicine field, multiple formulations have been developed and some have been successfully used in clinical applications due to CaPs capacity to substitute, repair, or regenerate bones and teeth and also for drug delivery systems. CaPs have become one of the most used classes of biocompatible and biodegradable materials. Hydroxyapatite offers excellent biocom-

patibility, bioactivity, low hardness, low compressive strength, and low density, while Hench's 45S5 Bioglass[®] has very low degradation and excellent bioactive properties. Even if numerous studies have been focused on developing a novel biomaterial with improved properties, only a limited number of studies provided in vitro and in vivo biocompatibility of substituted and co-substituted hydroxyapatite. A newer approach is the incorporation of multiple ions or another type of biomaterial and/or bioceramics into the structure of hydroxyapatite to form new types of composites with broader applications. With this aim, bioactive glasses are used in combination with hydroxyapatite for prevention of tissue damage, technology that is in continuous expansion. The bioactivity and the mechanical strength of bioglass are improved when it is reinforced with hydroxyapatite and, even more, with a combination of hydroxyapatite/other doping ions. Studies have been conducted to identify a different approach for the synthesis method with the appropriate composition of phases.

Because of the progress that has been made in material science and chemical industries, new perspectives for the use of CaPs appeared and one of the recent trends is using calcium phosphates in the cosmetic field as an alternative to potentially dangerous ingredients. Some general trends can also be anticipated. First of all, we expect that the scientific work in this field will be focused on improving CaPs properties and efficacy using various ion-doping methods, and not only based on hydroxyapatite, but also using different CaPs phases with different properties. Secondly, if we are considering the nanomedicine field, we should highlight the use of CaP nanoparticles for drug delivery. Ultimately, we anticipate that the principal sources of CaPs will be biogenic sources and byproducts, as sustainability is a keyword nowadays.

Author Contributions: Conceptualization; E.A. and D.G.F.; writing—original draft preparation; D.G.F. and A.V.P.; writing—review and editing, V.-A.S.; visualization, D.G.F. and V.-A.S.; supervision, E.A. All authors have read and agreed to the published version of the manuscript.

Funding: This research received no external funding.

Conflicts of Interest: The authors declare no conflict of interest.

References

1. Ishikawa, K.; Matsuya, S.; Miyamoto, Y.; Kawate, K. 9.05 Bioceramics. In *Bioengineering*; Elsevier Ltd.: Amsterdam, The Netherlands, 2007; pp. 169–214.
2. Riman, R.E.; Suchanek, W.L.; Byrappa, K.; Chen, C.-W.; Shuk, P.; Oakes, C.S. Solution Synthesis of Hydroxyapatite Designer Particulates. *Solid State Ion.* **2002**, *151*, 393–402. [[CrossRef](#)]
3. Cheng, K.; Weng, W.; Han, G.; Du, P.; Shen, G.; Yang, J.; Ferreira, J.M.F. The Effect of Triethanolamine on the Formation of Sol-Gel Derived Fluoroapatite/Hydroxyapatite Solid Solution. *J. Mater. Chem. Phys.* **2003**, *78*, 767–771. [[CrossRef](#)]
4. Weng, W.; Zhang, S.; Cheng, K.; Qu, H.; Du, P.; Shen, G.; Yuan, J.; Han, G. Sol-Gel Preparation of Bioactive Apatite Films. *Surf. Coat Technol.* **2003**, *167*, 292–296. [[CrossRef](#)]
5. Choi, D.; Marra, K.G.; Kumta, P.N. Chemical Synthesis of Hydroxyapatite/Poly(ϵ -Caprolactone) Composites. *Mater. Res. Bull.* **2004**, *39*, 417–432. [[CrossRef](#)]
6. Hench, L.L. Bioceramics: From Concept to Clinic. *J. Am. Ceram. Soc.* **1991**, *74*, 1487–1510. [[CrossRef](#)]
7. Gul, H.; Khan, M.; Khan, A.S. Bioceramics: Types and Clinical Applications. In *Handbook of Ionic Substituted Hydroxyapatites*; Elsevier: Amsterdam, The Netherlands, 2019; pp. 53–83. ISBN 9780081028346.
8. Das, A.; Pamu, D. A Comprehensive Review on Electrical Properties of Hydroxyapatite Based Ceramic Composites. *Mater. Sci. Eng. C* **2019**, *101*, 539–563. [[CrossRef](#)]
9. Habraken, W.; Habibovic, P.; Epple, M.; Bohner, M. Calcium Phosphates in Biomedical Applications: Materials for the Future? *Mater. Today* **2016**, *19*, 69–87. [[CrossRef](#)]
10. Hasegawa, M.; Doi, Y.; Uchida, A. Cell-Mediated Bioresorption of Sintered Carbonate Apatite in Rabbits. *J. Bone Jt. Surg.—Ser. B* **2003**, *85*, 142–147. [[CrossRef](#)]
11. Zhao, F.; Lei, B.; Li, X.; Mo, Y.; Wang, R.; Chen, D.; Chen, X. Promoting in Vivo Early Angiogenesis with Sub-Micrometer Strontium-Contained Bioactive Microspheres through Modulating Macrophage Phenotypes. *Biomaterials* **2018**, *178*, 36–47. [[CrossRef](#)]
12. Jones, J.R.; Gibson, I.R. Ceramics, Glasses, and Glass-Ceramics: Basic Principles. *Mater. Sci.* **2013**. [[CrossRef](#)]
13. Dasgupta, S.; Banerjee, S.S.; Bandyopadhyay, A.; Bose, S. Zn- and Mg-Doped Hydroxyapatite Nanoparticles for Controlled Release of Protein. *Langmuir* **2010**, *26*, 4958–4964. [[CrossRef](#)] [[PubMed](#)]

14. Tsai, S.W.; Huang, S.S.; Yu, W.X.; Hsu, Y.W.; Hsu, F.Y. Fabrication and Characteristics of Porous Hydroxyapatite-CaO Composite Nanofibers for Biomedical Applications. *Nanomaterials* **2018**, *8*, 570. [[CrossRef](#)] [[PubMed](#)]
15. Yilmaz, B.; Alshemary, A.Z.; Evis, Z. Co-Doped Hydroxyapatites as Potential Materials for Biomedical Applications. *Microchem. J.* **2019**, *144*, 443–453. [[CrossRef](#)]
16. Tomoda, K.; Ariizumi, H.; Nakaji, T.; Makino, K. Hydroxyapatite Particles as Drug Carriers for Proteins. *Colloids Surf. B Biointerfaces* **2010**, *76*, 226–235. [[CrossRef](#)]
17. Kester, M.; Heakal, Y.; Fox, T.; Sharma, A.; Robertson, G.P.; Morgan, T.T.; Altinoğlu, E.I.; Tabaković, A.; Parette, M.R.; Rouse, S.M.; et al. Calcium Phosphate Nanocomposite Particles for in Vitro Imaging and Encapsulated Chemotherapeutic Drug Delivery to Cancer Cells. *Nano Lett.* **2008**, *8*, 4116–4121. [[CrossRef](#)]
18. Bose, S.; Tarafder, S. Calcium Phosphate Ceramic Systems in Growth Factor and Drug Delivery for Bone Tissue Engineering: A Review. *Acta Biomater.* **2012**, *8*, 1401–1421. [[CrossRef](#)]
19. Salinas, A.J.; Vallet-Regí, M. Evolution of Ceramics with Medical Applications. *Z. Anorg. Allg. Chem.* **2007**, *633*, 1762–1773. [[CrossRef](#)]
20. Hench, L.L.; Splinter, R.J.; Allen, W.C.; Greenlee, T.K. Bonding Mechanisms at the Interface of Ceramic Prosthetic Materials. *J. Biomed. Mater. Res.* **1971**, *5*, 117–141. [[CrossRef](#)]
21. Zhao, X. Bioactive Materials in Orthopaedics. In *Bioactive Materials in Medicine: Design and Applications*; Elsevier Inc.: Amsterdam, The Netherlands, 2011; pp. 124–154. ISBN 9781845696245.
22. Fernando, S.; McEnery, M.; Guelcher, S.A. Polyurethanes for Bone Tissue Engineering. In *Advances in Polyurethane Biomaterials*; Elsevier Inc.: Amsterdam, The Netherlands, 2016; pp. 481–501. ISBN 9780081006221.
23. Balasubramaniam, B.; Prateek; Ranjan, S.; Saraf, M.; Kar, P.; Singh, S.P.; Thakur, V.K.; Singh, A.; Gupta, R.K. Antibacterial and Antiviral Functional Materials: Chemistry and Biological Activity toward Tackling COVID-19-like Pandemics. *ACS Pharm. Transl. Sci.* **2021**, *4*, 8–54. [[CrossRef](#)]
24. Park, J.; Um, S.H.; Seo, Y.; Lee, J.; Kim, Y.C.; Ok, M.R.; Hwang, S.W.; Sun, J.Y.; Han, H.S.; Jeon, H. Improving Hydroxyapatite Coating Ability on Biodegradable Metal through Laser-Induced Hydrothermal Coating in Liquid Precursor: Application in Orthopedic Implants. *Bioact. Mater.* **2022**. [[CrossRef](#)]
25. Furko, M.; Horváth, Z.E.; Sulyok, A.; Kis, V.K.; Balázs, K.; Mihály, J.; Balázs, C. Preparation and Morphological Investigation on Bioactive Ion-Modified Carbonated Hydroxyapatite-Biopolymer Composite Ceramics as Coatings for Orthopaedic Implants. *Ceram. Int.* **2022**, *48*, 760–768. [[CrossRef](#)]
26. Hikku, G.S.; Arthi, C.; Jeen Robert, R.B.; Jeyasubramanian, K.; Murugesan, R. Calcium Phosphate Conversion Technique: A Versatile Route to Develop Corrosion Resistant Hydroxyapatite Coating over Mg/Mg Alloys Based Implants. *J. Magnes. Alloy.* **2022**, *10*, 1821–1845. [[CrossRef](#)]
27. Nagai, M.; Nishino, T. Surface conduction of porous hydroxyapatite cellaa'viics at elevated temperatures. *Solid State Ion.* **1988**, *28–30*, 1456–1461. [[CrossRef](#)]
28. Suchanek, W.L.; Byrappa, K.; Shuk, P.; Riman, R.E.; Janas, V.F.; Tenhuisen, K.S. Mechanochemical-Hydrothermal Synthesis of Calcium Phosphate Powders with Coupled Magnesium and Carbonate Substitution. *J. Solid State Chem.* **2004**, *177*, 793–799. [[CrossRef](#)]
29. Chahkandi, M. Mechanism of Congo Red Adsorption on New Sol-Gel-Derived Hydroxyapatite Nano-Particle. *Mater. Chem. Phys.* **2017**, *202*, 340–351. [[CrossRef](#)]
30. Bohner, M. Calcium Orthophosphates in Medicine: From Ceramics to Calcium Phosphate Cements. *Injury* **2000**, *31*, D37–D47. [[CrossRef](#)]
31. Roy, I.; Mitra, S.; Maitra, A.; Mozumdar, S. Calcium Phosphate Nanoparticles as Novel Non-Viral Vectors for Targeted Gene Delivery. *Int. J. Pharm.* **2003**, *250*, 25–33. [[CrossRef](#)]
32. Lai, C.; Tang, S.Q.; Wang, Y.J.; Wei, K. Formation of Calcium Phosphate Nanoparticles in Reverse Microemulsions. *Mater. Lett.* **2005**, *59*, 210–214. [[CrossRef](#)]
33. Talal, A.; Hamid, S.K.; Khan, M.; Khan, A.S. Structure of Biological Apatite: Bone and Tooth. In *Handbook of Ionic Substituted Hydroxyapatites*; Elsevier: Amsterdam, The Netherlands, 2019; pp. 1–19. ISBN 9780081028346.
34. Koutsopoulos, S. Synthesis and Characterization of Hydroxyapatite Crystals: A Review Study on the Analytical Methods. *J. Biomed. Mater. Res.* **2002**, *62*, 600–612. [[CrossRef](#)]
35. Doi, Y.; Shibutani, T.; Moriwaki, Y.; Kajimoto, T.; Iwayama, Y. Sintered Carbonate Apatites as Bioresorbable Bone Substitutes. *J. Biomed. Mater. Res.* **1998**, *39*, 603–610. [[CrossRef](#)]
36. Nachtigall, P.; Arean, C.O. Themed Issue on Characterization of Adsorbed Species. *Phys. Chem. Chem. Phys.* **2010**, *12*, 6307–6308. [[CrossRef](#)] [[PubMed](#)]
37. Mostafa, N.Y.; Brown, P.W. Computer Simulation of Stoichiometric Hydroxyapatite: Structure and Substitutions. *J. Phys. Chem. Solids* **2007**, *68*, 431–437. [[CrossRef](#)]
38. Mondal, S.; Dorozhkin, S.V.; Pal, U. Recent Progress on Fabrication and Drug Delivery Applications of Nanostructured Hydroxyapatite. *Wiley Interdiscip. Rev. Nanomed. Nanobiotechnol.* **2018**, *10*, 1504. [[CrossRef](#)] [[PubMed](#)]
39. Fernandez, E.; Gil, F.J.; Ginebra, M.P.; Driessens, F.C.M.; Planell, J.A.; Best, S.M. Calcium Phosphate Bone Cements for Clinical Applications Part II: Precipitate Formation during Setting Reactions. *J. Mater. Sci. Mater. Med.* **1999**, *10*, 177–183. [[CrossRef](#)] [[PubMed](#)]

40. Sadat-Shojai, M.; Khorasani, M.T.; Dinpanah-Khoshdargi, E.; Jamshidi, A. Synthesis Methods for Nanosized Hydroxyapatite with Diverse Structures. *Acta Biomater.* **2013**, *9*, 7591–7621. [[CrossRef](#)]
41. Zhang, Y.; Lu, J. The Transformation of Single-Crystal Calcium Phosphate Ribbon-like Fibres to Hydroxyapatite Spheres Assembled from Nanorods. *Nanotechnology* **2008**, *19*, 155608. [[CrossRef](#)]
42. Tas, A.C. Synthesis of Biomimetic Ca-Hydroxyapatite Powders at 373C in Synthetic Body fluids. *Biomaterials* **2000**, *21*, 1429–1438.
43. Mobasherpour, I.; Heshajin, M.S.; Kazemzadeh, A.; Zakeri, M. Synthesis of Nanocrystalline Hydroxyapatite by Using Precipitation Method. *J. Alloys Compd.* **2007**, *430*, 330–333. [[CrossRef](#)]
44. Padmanabhan, S.K.; Balakrishnan, A.; Chu, M.C.; Lee, Y.J.; Kim, T.N.; Cho, S.J. Sol-Gel Synthesis and Characterization of Hydroxyapatite Nanorods. *Particuology* **2009**, *7*, 466–470. [[CrossRef](#)]
45. Szterner, P.; Biernat, M. The Synthesis of Hydroxyapatite by Hydrothermal Process with Calcium Lactate Pentahydrate: The Effect of Reagent Concentrations, pH, Temperature, and Pressure. *Bioinorg. Chem. Appl.* **2022**, *2022*, 3481677. [[CrossRef](#)]
46. Cihlar, J.; Castkova, K. Direct Synthesis of Nanocrystalline Hydroxyapatite by Hydrothermal Hydrolysis of Alkylphosphates. *Mon. Für Chem.-Chem. Mon.* **2002**, *133*, 761–771. [[CrossRef](#)]
47. Zhou, W.Y.; Wang, M.; Cheung, W.L.; Guo, B.C.; Jia, D.M. Synthesis of Carbonated Hydroxyapatite Nanospheres through Nanoemulsion. *J. Mater. Sci. Mater. Med.* **2008**, *19*, 103–110. [[CrossRef](#)] [[PubMed](#)]
48. Vukomanović, M.; Bračko, I.; Poljanšek, I.; Uskoković, D.; Škapin, S.D.; Suvorov, D. The Growth of Silver Nanoparticles and Their Combination with Hydroxyapatite to Form Composites via a Sonochemical Approach. *Cryst. Growth Des.* **2011**, *11*, 3802–3812. [[CrossRef](#)]
49. Ekka, B.; Nayak, S.R.; Achary, L.S.K.; Sarita; Kumar, A.; Mawatwal, S.; Dhiman, R.; Dash, P.; Patel, R.K. Synthesis of Hydroxyapatite-Zirconia Nanocomposite through Sonochemical Route: A Potential Catalyst for Degradation of Phenolic Compounds. *J. Environ. Chem. Eng.* **2018**, *6*, 6504–6515. [[CrossRef](#)]
50. Jevtić, M.; Mitrić, M.; Škapin, S.; Jančar, B.; Ignjatović, N.; Uskoković, D. Crystal Structure of Hydroxyapatite Nanorods Synthesized by Sonochemical Homogeneous Precipitation. *Cryst. Growth Des.* **2008**, *8*, 2217–2222. [[CrossRef](#)]
51. Sahni, G.; Gopinath, P.; Jeevanandam, P. A Novel Thermal Decomposition Approach to Synthesize Hydroxyapatite-Silver Nanocomposites and Their Antibacterial Action against GFP-Expressing Antibiotic Resistant *E. coli*. *Colloids Surf. B Biointerfaces* **2013**, *103*, 441–447. [[CrossRef](#)]
52. Barralet, J.; Knowles, J.C.; Best, S.; Bonfield, W. Thermal Decomposition of Synthesised Carbonate Hydroxyapatite. *J. Mater. Sci. Mater. Med.* **2002**, *13*, 529–533. [[CrossRef](#)]
53. Chun, Y.A.N.G.; Guo, Y.K.; Zhang, M.L. Thermal Decomposition and Mechanical Properties of Hydroxyapatite Ceramic. *Trans. Nonferrous Met. Soc. China* **2010**, *20*, 254–258. [[CrossRef](#)]
54. Obada, D.O.; Salami, K.A.; Oyedepi, A.N.; Fasanya, O.O.; Suleiman, M.U.; Ibisola, B.A.; Atta, A.Y.; Doodoo-Arhin, D.; Kuburi, L.S.; Dauda, M.; et al. Solution Combustion Synthesis of Strontium-Doped Hydroxyapatite: Effect of Sintering and Low Compaction Pressure on the Mechanical Properties and Physiological Stability. *Mater. Lett.* **2021**, *304*, 130613. [[CrossRef](#)]
55. Ghosh, S.K.; Roy, S.K.; Kundu, B.; Datta, S.; Basu, D. Synthesis of Nano-Sized Hydroxyapatite Powders through Solution Combustion Route under Different Reaction Conditions. *Mater. Sci. Eng. B Solid State Mater. Adv. Technol.* **2011**, *176*, 14–21. [[CrossRef](#)]
56. Taş, A.C. Molten Salt Synthesis of Calcium Hydroxyapatite Whiskers. *J. Am. Ceram. Soc.* **2001**, *84*, 295–300. [[CrossRef](#)]
57. Zhang, H.G.; Zhu, Q. Preparation of Fluoride-Substituted Hydroxyapatite by a Molten Salt Synthesis Route. *J. Mater. Sci. Mater. Med.* **2006**, *17*, 691–695. [[CrossRef](#)] [[PubMed](#)]
58. Mondal, S.; Pal, U.; Dey, A. Natural Origin Hydroxyapatite Scaffold as Potential Bone Tissue Engineering Substitute. *Ceram. Int.* **2016**, *42*, 18338–18346. [[CrossRef](#)]
59. Sobczak, A.; Kida, A.; Kowalski, Z.; Wzorek, Z. Evaluation of the Biomedical Properties of Hydroxyapatite Obtained from Bone Waste. *Pol. J. Chem. Technol.* **2009**, *11*, 37–43. [[CrossRef](#)]
60. Wu, S.C.; Tsou, H.K.; Hsu, H.C.; Hsu, S.K.; Liou, S.P.; Ho, W.F. A Hydrothermal Synthesis of Eggshell and Fruit Waste Extract to Produce Nanosized Hydroxyapatite. *Ceram. Int.* **2013**, *39*, 8183–8188. [[CrossRef](#)]
61. Charlena; Suparto, I.H.; Putri, D.K. Synthesis of Hydroxyapatite from Rice Fields Snail Shell (*Bellamya Javanica*) through Wet Method and Pore Modification Using Chitosan. *Procedia Chem.* **2015**, *17*, 27–35. [[CrossRef](#)]
62. Vallet-Regí, M.; González-Calbet, J.M. Calcium Phosphates as Substitution of Bone Tissues. *Prog. Solid State Chem.* **2004**, *32*, 1–31. [[CrossRef](#)]
63. Chirică, I.M.; Enciu, A.M.; Tite, T.; Dudău, M.; Albulescu, L.; Iconaru, S.L.; Predoi, D.; Pasuk, I.; Enculescu, M.; Radu, C.; et al. The Physico-Chemical Properties and Exploratory Real-Time Cell Analysis of Hydroxyapatite Nanopowders Substituted with Ce, Mg, Sr, and Zn (0.5–5 at.%). *Materials* **2021**, *14*, 3808. [[CrossRef](#)]
64. Vallet-Regí, M.; Arcos, D. Silicon Substituted Hydroxyapatites. A Method to Upgrade Calcium Phosphate Based Implants. *J. Mater. Chem.* **2005**, *15*, 1509–1516. [[CrossRef](#)]
65. Gibson, I.R.; Best, S.M.; Bonfield, W. Chemical Characterization of Silicon-Substituted Hydroxyapatite. *J. Biomed. Mater. Res.* **1999**, *15*, 422–428. [[CrossRef](#)]
66. Uskoković, V. Ion-Doped Hydroxyapatite: An Impasse or the Road to Follow? *Ceram. Int.* **2020**, *46*, 11443–11465. [[CrossRef](#)]
67. Wopenka, B.; Pasteris, J.D. A Mineralogical Perspective on the Apatite in Bone. *Mater. Sci. Eng. C* **2005**, *25*, 131–143. [[CrossRef](#)]

68. Boanini, E.; Gazzano, M.; Bigi, A. Ionic Substitutions in Calcium Phosphates Synthesized at Low Temperature. *Acta Biomater.* **2010**, *6*, 1882–1894. [[CrossRef](#)] [[PubMed](#)]
69. Matsunaga, K. First-Principles Study of Substitutional Magnesium and Zinc in Hydroxyapatite and Octacalcium Phosphate. *J. Chem. Phys.* **2008**, *128*, 06B618. [[CrossRef](#)] [[PubMed](#)]
70. Sprio, S.; Dapporto, M.; Preti, L.; Mazzoni, E.; Iaquinta, M.R.; Martini, F.; Tognon, M.; Pugno, N.M.; Restivo, E.; Visai, L.; et al. Enhancement of the Biological and Mechanical Performances of Sintered Hydroxyapatite by Multiple Ions Doping. *Front. Mater.* **2020**, *7*, 224. [[CrossRef](#)]
71. Salam, N.; Gibson, I.R. Lithium Ion Doped Carbonated Hydroxyapatite Compositions: Synthesis, Physicochemical Characterisation and Effect on Osteogenic Response in Vitro. *Biomater. Adv.* **2022**, *140*, 213068. [[CrossRef](#)]
72. Li, H.; Zhao, X.; Cao, S.; Li, K.; Chen, M.; Xu, Z.; Lu, J.; Zhang, L. Na-Doped Hydroxyapatite Coating on Carbon/Carbon Composites: Preparation, in Vitro Bioactivity and Biocompatibility. *Appl. Surf. Sci.* **2012**, *263*, 163–173. [[CrossRef](#)]
73. Riaz, M.; Zia, R.; Ijaz, A.; Hussain, T.; Mohsin, M.; Malik, A. Synthesis of Monophasic Ag Doped Hydroxyapatite and Evaluation of Antibacterial Activity. *Mater. Sci. Eng. C* **2018**, *90*, 308–313. [[CrossRef](#)]
74. Jelinek, M.; Kocourek, T.; Remsa, J.; Weiserová, M.; Jurek, K.; Mikšovský, J.; Strnad, J.; Galandáková, A.; Ulrichová, J. Antibacterial, Cytotoxicity and Physical Properties of Laser—Silver Doped Hydroxyapatite Layers. *Mater. Sci. Eng. C* **2013**, *33*, 1242–1246. [[CrossRef](#)]
75. Predoi, D.; Iconaru, S.L.; Predoi, M.V.; Stan, G.E.; Buton, N. Synthesis, Characterization, and Antimicrobial Activity of Magnesium-Doped Hydroxyapatite Suspensions. *Nanomaterials* **2019**, *9*, 1295. [[CrossRef](#)]
76. Zhou, Y.; Li, W.; Jiang, X.; Sun, Y.; Yang, H.; Liu, Q.; Cao, Y.; Zhang, Y.; Cheng, H. Synthesis of Strontium (Sr) Doped Hydroxyapatite (HAp) Nanorods for Enhanced Adsorption of Cr (VI) Ions from Wastewater. *Ceram. Int.* **2021**, *47*, 16730–16736. [[CrossRef](#)]
77. de Lima, C.O.; de Oliveira, A.L.M.; Chantelle, L.; Silva Filho, E.C.; Jaber, M.; Fonseca, M.G. Zn-Doped Mesoporous Hydroxyapatites and Their Antimicrobial Properties. *Colloids Surf. B Biointerfaces* **2021**, *198*, 111471. [[CrossRef](#)] [[PubMed](#)]
78. Fan, Q.; Fan, F.; Xu, W.; Zhang, H.; Liu, N. The Structural and Surface Properties of Al-Doped Hydroxyapatite (Ca₅(PO₄)₃OH) Nanorods and Their Applications for PH-Induced Drug Delivery. *J. Alloy. Compd.* **2021**, *879*, 160414. [[CrossRef](#)]
79. Kolesnikov, I.E.; Nikolaev, A.M.; Lähderanta, E.; Frank-Kamenetskaya, O.V.; Kuz'mina, M.A. Structural and Luminescence Properties of Ce³⁺-Doped Hydroxyapatite Nanocrystalline Powders. *Opt. Mater.* **2020**, *99*, 109550. [[CrossRef](#)]
80. Vladescu, A.; Padmanabhan, S.C.; Ak Azem, F.; Braic, M.; Titorencu, I.; Birlik, I.; Morris, M.A.; Braic, V. Mechanical Properties and Biocompatibility of the Sputtered Ti Doped Hydroxyapatite. *J. Mech. Behav. Biomed. Mater.* **2016**, *63*, 314–325. [[CrossRef](#)]
81. Xu, D.; Xu, Z.; Cheng, L.; Gao, X.; Sun, J.; Chen, L. Improvement of the Mechanical Properties and Osteogenic Activity of 3D-Printed Polylactic Acid Porous Scaffolds by Nano-Hydroxyapatite and Nano-Magnesium Oxide. *Heliyon* **2022**, *8*, e09748. [[CrossRef](#)]
82. Li, C.; Qin, W.; Lakshmanan, S.; Ma, X.; Sun, X.; Xu, B. Hydroxyapatite Based Biocomposite Scaffold: A Highly Biocompatible Material for Bone Regeneration. *Saudi J. Biol. Sci.* **2020**, *27*, 2143–2148. [[CrossRef](#)]
83. Farzadi, A.; Bakhshi, F.; Solati-Hashjin, M.; Asadi-Eydivand, M.; Osman, N.A.A. Magnesium Incorporated Hydroxyapatite: Synthesis and Structural Properties Characterization. *Ceram. Int.* **2014**, *40*, 6021–6029. [[CrossRef](#)]
84. Cacciotti, I.; Bianco, A.; Lombardi, M.; Montanaro, L. Mg-Substituted Hydroxyapatite Nanopowders: Synthesis, Thermal Stability and Sintering Behaviour. *J. Eur. Ceram. Soc.* **2009**, *29*, 2969–2978. [[CrossRef](#)]
85. Bauer, L.; Antunović, M.; Rogina, A.; Ivanković, M.; Ivanković, H. Bone-Mimetic Porous Hydroxyapatite/Whitlockite Scaffolds: Preparation, Characterization and Interactions with Human Mesenchymal Stem Cells. *J. Mater. Sci.* **2021**, *56*, 3947–3969. [[CrossRef](#)]
86. Aina, V.; Lusvardi, G.; Annaz, B.; Gibson, I.R.; Imrie, F.E.; Malavasi, G.; Menabue, L.; Cerrato, G.; Martra, G. Magnesium- and Strontium-Co-Substituted Hydroxyapatite: The Effects of Doped-Ions on the Structure and Chemico-Physical Properties. *J. Mater. Sci. Mater. Med.* **2012**, *23*, 2867–2879. [[CrossRef](#)] [[PubMed](#)]
87. Predoi, D.; Iconaru, S.L.; Predoi, M.V.; Motelica-Heino, M.; Buton, N.; Megier, C. Obtaining and Characterizing Thin Layers of Magnesium Doped Hydroxyapatite by Dip Coating Procedure. *Coatings* **2020**, *10*, 510. [[CrossRef](#)]
88. Ito, A.; Kawamura, H.; Otsuka, M.; Ikeuchi, M.; Ohgushi, H.; Ishikawa, K.; Onuma, K.; Kanzaki, N.; Sogo, Y.; Ichinose, N. Zinc-Releasing Calcium Phosphate for Stimulating Bone Formation. *Mater. Sci. Eng. C* **2002**, *22*, 21–25. [[CrossRef](#)]
89. Tang, Y.; Chappell, H.F.; Dove, M.T.; Reeder, R.J.; Lee, Y.J. Zinc Incorporation into Hydroxylapatite. *Biomaterials* **2009**, *30*, 2864–2872. [[CrossRef](#)] [[PubMed](#)]
90. Ressler, A.; Žužič, A.; Ivanišević, I.; Kamboj, N.; Ivanković, H. Ionic Substituted Hydroxyapatite for Bone Regeneration Applications: A Review. *Open Ceram.* **2021**, *6*, 100122. [[CrossRef](#)]
91. Ofudje, E.A.; Adeogun, A.I.; Idowu, M.A.; Kareem, S.O. Synthesis and Characterization of Zn-Doped Hydroxyapatite: Scaffold Application, Antibacterial and Bioactivity Studies. *Heliyon* **2019**, *5*, e01716. [[CrossRef](#)]
92. Predoi, D.; Iconaru, S.L.; Ciobanu, S.C.; Predoi, S.A.; Buton, N.; Megier, C.; Beuran, M. Development of Iron-Doped Hydroxyapatite Coatings. *Coatings* **2021**, *11*, 186. [[CrossRef](#)]
93. Jose, S.; Senthilkumar, M.; Elayaraja, K.; Haris, M.; George, A.; Raj, A.D.; Sundaram, S.J.; Bashir, A.K.H.; Maaza, M.; Kaviyarasu, K. Preparation and Characterization of Fe Doped N-Hydroxyapatite for Biomedical Application. *Surf. Interfaces* **2021**, *25*, 101185. [[CrossRef](#)]

94. Cacciotti, I. Cationic and Anionic Substitutions in Hydroxyapatite. In *Handbook of Bioceramics and Biocomposites*; Springer International Publishing: Berlin/Heidelberg, Germany, 2015; pp. 1–68.
95. Paduraru, A.V.; Musuc, A.M.; Oprea, O.C.; Trusca, R.; Iordache, F.; Vasile, B.S.; Andronescu, E. Synthesis and Characterization of Photoluminescent Ce(III) and Ce(IV) Substituted Hydroxyapatite Nanomaterials by Co-Precipitation Method: Cytotoxicity and Biocompatibility Evaluation. *Nanomaterials* **2021**, *11*, 1911. [[CrossRef](#)]
96. Phatai, P.; Futalan, C.M.; Utara, S.; Khemthong, P.; Kamonwannasit, S. Structural Characterization of Cerium-Doped Hydroxyapatite Nanoparticles Synthesized by an Ultrasonic-Assisted Sol-Gel Technique. *Results Phys.* **2018**, *10*, 956–963. [[CrossRef](#)]
97. Kanchana, P.; Navaneethan, M.; Sekar, C. Fabrication of Ce Doped Hydroxyapatite Nanoparticles Based Non-Enzymatic Electrochemical Sensor for the Simultaneous Determination of Norepinephrine, Uric Acid and Tyrosine. *Mater. Sci. Eng. B Solid State Mater. Adv. Technol.* **2017**, *226*, 132–140. [[CrossRef](#)]
98. Kaygili, O.; Dorozhkin, S.V.; Keser, S. Synthesis and Characterization of Ce-Substituted Hydroxyapatite by Sol-Gel Method. *Mater. Sci. Eng. C* **2014**, *42*, 78–82. [[CrossRef](#)] [[PubMed](#)]
99. Gopi, D.; Ramya, S.; Rajeswari, D.; Karthikeyan, P.; Kavitha, L. Strontium, Cerium Co-Substituted Hydroxyapatite Nanoparticles: Synthesis, Characterization, Antibacterial Activity towards Prokaryotic Strains and in Vitro Studies. *Colloids Surf. A Phys. Eng. Asp.* **2014**, *451*, 172–180. [[CrossRef](#)]
100. Sanosh, K.P.; Chu, M.-C.; Balakrishnan, A.; Kim, T.N.; Cho, S.-J. Preparation and Characterization of Nano-Hydroxyapatite Powder Using Sol-Gel Technique. *Bull. Mater. Sci.* **2009**, *32*, 465–470. [[CrossRef](#)]
101. Stoica, T.F.; Morosanu, C.; Slav, A.; Stoica, T.; Osiceanu, P.; Anastasescu, C.; Gartner, M.; Zaharescu, M. Hydroxyapatite Films Obtained by Sol-Gel and Sputtering. *Thin Solid Film.* **2008**, *516*, 8112–8116. [[CrossRef](#)]
102. Amjad, Z. *Calcium Phosphates in Biological and Industrial Systems*; Springer: Berlin/Heidelberg, Germany, 1998.
103. Rogers, K.D.; Daniels, P. An X-Ray Diffraction Study of the Effects of Heat Treatment on Bone Mineral Microstructure. *Biomaterials* **2002**, *23*, 2577–2585. [[CrossRef](#)]
104. Merry, J.C.; Gibson, I.R.; Best, S.M.; Bonfield, W. Synthesis and Characterization of Carbonate Hydroxyapatite. *J. Mater. Sci. Mater. Med.* **1998**, *9*, 779–783. [[CrossRef](#)]
105. El Feki, E.; Savariault, J.M.; Salah, A.B. Structure Refinements by the Rietveld Method of Partially Substituted: $\text{Ca}_9\text{Na}_{0.5}(\text{PO}_4)_4(\text{CO}_3)_{1.5}(\text{OH})_2$. *J. Alloy. Compd.* **1999**, *287*, 114–120. [[CrossRef](#)]
106. Lala, S.; Brahmachari, S.; Das, P.K.; Das, D.; Kar, T.; Pradhan, S.K. Biocompatible Nanocrystalline Natural Bonelike Carbonated Hydroxyapatite Synthesized by Mechanical Alloying in a Record Minimum Time. *Mater. Sci. Eng. C* **2014**, *42*, 647–656. [[CrossRef](#)]
107. Šupová, M. Substituted Hydroxyapatites for Biomedical Applications: A Review. *Ceram. Int.* **2015**, *41*, 9203–9231. [[CrossRef](#)]
108. Hesaraki, S.; Nazarian, H.; Pourbaghi-Masouleh, M.; Borhan, S. Comparative Study of Mesenchymal Stem Cells Osteogenic Differentiation on Low-Temperature Biomineralized Nanocrystalline Carbonated Hydroxyapatite and Sintered Hydroxyapatite. *J. Biomed. Mater. Res. B Appl. Biomater.* **2014**, *102*, 108–118. [[CrossRef](#)] [[PubMed](#)]
109. Germaini, M.M.; Detsch, R.; Grünewald, A.; Magnaudeix, A.; Lalloue, F.; Boccacini, A.R.; Champion, E. Osteoblast and Osteoclast Responses to A/B Type Carbonate-Substituted Hydroxyapatite Ceramics for Bone Regeneration. *Biomed. Mater.* **2017**, *12*, 035008. [[CrossRef](#)] [[PubMed](#)]
110. Spence, G.; Patel, N.; Brooks, R.; Rushton, N. Carbonate Substituted Hydroxyapatite: Resorption by Osteoclasts Modifies the Osteoblastic Response. *J. Biomed. Mater. Res. A* **2009**, *90*, 217–224. [[CrossRef](#)] [[PubMed](#)]
111. Uysal, I.; Severcan, F.; Evis, Z. Structural and Mechanical Characteristics of Nanohydroxyapatite Doped with Zinc and Chloride. *Adv. Appl. Ceram.* **2013**, *112*, 149–157. [[CrossRef](#)]
112. Gomes, S.; Nedelec, J.M.; Jallot, E.; Sheptyakov, D.; Renaudin, G. Unexpected Mechanism of Zn^{2+} Insertion in Calcium Phosphate Bioceramics. *Chem. Mater.* **2011**, *23*, 3072–3085. [[CrossRef](#)]
113. Basar, B.; Tezcaner, A.; Keskin, D.; Evis, Z. Improvements in Microstructural, Mechanical, and Biocompatibility Properties of Nano-Sized Hydroxyapatites Doped with Yttrium and Fluoride. *Ceram. Int.* **2010**, *36*, 1633–1643. [[CrossRef](#)]
114. Basar, B.; Evis, Z. Structural Investigation of Nanohydroxyapatite Doped with Y^{3+} and F^- Ions. *Mater. Sci. Technol.* **2009**, *25*, 794–798. [[CrossRef](#)]
115. Evis, Z.; Basar, B.; Sun, Z.P. Diametral Strength Testing of Hydroxyapatites Doped with Yttrium and Fluoride. *Adv. Appl. Ceram.* **2010**, *109*, 383–388. [[CrossRef](#)]
116. Yilmaz, B.; Evis, Z. Raman Spectroscopy Investigation of Nano Hydroxyapatite Doped with Yttrium and Fluoride Ions. *Spectrosc. Lett.* **2014**, *47*, 24–29. [[CrossRef](#)]
117. Tahmasebifar, A.; Evis, Z. Structural and Mechanical Characteristics of Hydroxyapatite and Tri-Calcium Phosphates Doped with Al^{3+} and F^- Ions. *J. Ceram. Process. Res.* **2013**, *14*, 549–556. [[CrossRef](#)]
118. İnce, T.; Kaygili, O.; Tatar, C.; Bulut, N.; Koytepe, S.; Ates, T. The Effects of Ni-Addition on the Crystal Structure, Thermal Properties and Morphology of Mg-Based Hydroxyapatites Synthesized by a Wet Chemical Method. *Ceram. Int.* **2018**, *44*, 14036–14043. [[CrossRef](#)]
119. Alshemary, A.Z.; Engin Pazarceviren, A.; Tezcaner, A.; Evis, Z. $\text{Fe}^{3+}/\text{SeO}_4^{2-}$ Dual Doped Nano Hydroxyapatite: A Novel Material for Biomedical Applications. *J. Biomed. Mater. Res. B Appl. Biomater.* **2018**, *106*, 340–352. [[CrossRef](#)] [[PubMed](#)]
120. Laskus, A.; Zgadzaj, A.; Kolmas, J. Zn^{2+} and SeO_3^{2-} Co-Substituted Hydroxyapatite: Physicochemical Properties and Biological Usefulness. *Ceram. Int.* **2019**, *45*, 22707–22715. [[CrossRef](#)]

121. Ahmed, M.K.; Mansour, S.F.; Mostafa, M.S.; Darwesh, R.; El-dek, S.I. Structural, Mechanical and Thermal Features of Bi and Sr Co-Substituted Hydroxyapatite. *J. Mater. Sci.* **2019**, *54*, 1977–1991. [[CrossRef](#)]
122. Huang, Y.; Zhang, X.; Mao, H.; Li, T.; Zhao, R.; Yan, Y.; Pang, X. Osteoblastic Cell Responses and Antibacterial Efficacy of Cu/Zn Co-Substituted Hydroxyapatite Coatings on Pure Titanium Using Electrodeposition Method. *RSC Adv.* **2015**, *5*, 17076–17086. [[CrossRef](#)]
123. Stanić, V.; Janačković, D.; Dimitrijević, S.; Tanasković, S.B.; Mitrić, M.; Pavlović, M.S.; Krstić, A.; Jovanović, D.; Raičević, S. Synthesis of Antimicrobial Monophase Silver-Doped Hydroxyapatite Nanopowders for Bone Tissue Engineering. *Appl. Surf. Sci.* **2011**, *257*, 4510–4518. [[CrossRef](#)]
124. Li, P.; Jia, Z.; Wang, Q.; Tang, P.; Wang, M.; Wang, K.; Fang, J.; Zhao, C.; Ren, F.; Ge, X.; et al. A Resilient and Flexible Chitosan/Silk Cryogel Incorporated Ag/Sr Co-Doped Nanoscale Hydroxyapatite for Osteoinductivity and Antibacterial Properties. *J. Mater. Chem. B* **2018**, *6*, 7427–7438. [[CrossRef](#)]
125. Zhang, X.; Wang, B.; Ma, L.; Xie, L.; Yang, H.; Li, Y.; Wang, S.; Qiao, H.; Lin, H.; Lan, J.; et al. Chemical Stability, Antibacterial and Osteogenic Activities Study of Strontium-Silver Co-Substituted Fluorohydroxyapatite Nanopillars: A Potential Multifunctional Biological Coating. *Ceram. Int.* **2020**, *46*, 27758–27773. [[CrossRef](#)]
126. Hu, C.; Guo, J.; Qu, J.; Hu, X. Efficient Destruction of Bacteria with Ti(IV) and Antibacterial Ions in Co-Substituted Hydroxyapatite Films. *Appl. Catal. B* **2007**, *73*, 345–353. [[CrossRef](#)]
127. Ullah, I.; Siddiqui, M.A.; Kolawole, S.K.; Liu, H.; Zhang, J.; Ren, L.; Yang, K. Synthesis, Characterization and in Vitro Evaluation of Zinc and Strontium Binary Doped Hydroxyapatite for Biomedical Application. *Ceram. Int.* **2020**, *46*, 14448–14459. [[CrossRef](#)]
128. Lim, P.N.; Konishi, T.; Wang, Z.; Feng, J.; Wang, L.; Han, J.; Yang, Z.; Thian, E.S. Enhancing Osteoconductivity and Biocompatibility of Silver-Substituted Apatite in Vivo through Silicon Co-Substitution. *Mater. Lett.* **2018**, *212*, 90–93. [[CrossRef](#)]
129. Balamurugan, A.; Balossier, G.; Kannan, S.; Michel, J.; Rebelo, A.H.S.; Ferreira, J.M.F. Development and in Vitro Characterization of Sol-Gel Derived CaO-P₂O₅-SiO₂-ZnO Bioglass. *Acta Biomater.* **2007**, *3*, 255–262. [[CrossRef](#)] [[PubMed](#)]
130. Beckham, C.A.; Greenlee, T.K., Jr.; Crebo, A.R. Bone Formation at a Ceramic Implant Interface. *Calcif. Tissue Int.* **1971**, *8*, 165–171. [[CrossRef](#)] [[PubMed](#)]
131. Griss, P.; Greenspan, D.C.; Heimke, G.; Krempien, B.; Buchinger, R.; Hench, L.L.; Jentschura, G. Evaluation of a Bioglass-Coated Al₂O₃ Total Hip Prosthesis in Sheep. *J. Biomed. Mater. Res.* **1976**, *10*, 511–518. [[CrossRef](#)]
132. Hench, L.L. Chronology of Bioactive Glass Development and Clinical Applications. *New J. Glass Ceram.* **2013**, *03*, 67–73. [[CrossRef](#)]
133. Wilson, J.; Pigott, G.H.; Schoent, F.J.; Hench, L.L. Toxicology and Biocompatibility of Bioglasses. *J. Biomed. Mater. Res.* **1981**, *15*, 805–817. [[CrossRef](#)]
134. Stanley, H.R.; Hench, L.; Going, R.; Bennett, C.; Chellemi, S.J.; King, C.; Ingersoll, N.; Ethridge, E.; Kreutziger, K. The Implantation of Natural Tooth Form Bioglasses in Baboons A Preliminary Report. *Oral Surg. Oral Med. Oral Pathol.* **1976**, *42*, 339–356. [[CrossRef](#)]
135. Stanley, H.R.; Hall, M.B.; Colaizzi, F.; Clark, A.E. Residual Alveolar Ridge Maintenance with a New Endosseous Implant Material. *J. Prosthet. Dent.* **1987**, *58*, 607–613. [[CrossRef](#)]
136. Hench, L.L.; West, J.K. The Sol-Gel Process. *Chem. Rev.* **1990**, *90*, 33–72. [[CrossRef](#)]
137. Li, R.; Clark, A.E.; Hench, L.L. An Investigation of Bioactive Glass Powders by Sol-Gel Processing. *J. Appl. Biomater.* **1991**, *2*, 231–239. [[CrossRef](#)]
138. Baino, F.; Hamzehlou, S.; Kargozar, S. Bioactive Glasses: Where Are We and Where Are We Going? *J. Funct. Biomater.* **2018**, *9*, 25. [[CrossRef](#)] [[PubMed](#)]
139. Hench, L.L.; Polka, J.M.; Xynos, I.D.; Buttery, L.D.K. Bioactive Materials to Control Cell Cycle. *Mat. Res. Innov.* **2000**, *3*, 313–323. [[CrossRef](#)]
140. Jones, J.R. Bioactive Glasses. In *Bioceramics and Their Clinical Applications*; Elsevier Inc.: Amsterdam, The Netherlands, 2008; pp. 266–283. ISBN 9781845692049.
141. Sepulveda, P.; Jones, J.R.; Hench, L.L. Characterization of Melt-Derived 45S5 and Sol-Gel-Derived 58S Bioactive Glasses. *J. Biomed. Mater. Res.* **2001**, *58*, 734–740. [[CrossRef](#)] [[PubMed](#)]
142. Yu, J.; Arai, Y.; Masaki, T.; Ishikawa, T.; Yoda, S.; Kohara, S.; Taniguchi, H.; Itoh, M.; Kuroiwa, Y. Fabrication of BaTi₂O₅ Glass-Ceramics with Unusual Dielectric Properties during Crystallization. *Chem. Mater.* **2006**, *18*, 2169–2173. [[CrossRef](#)]
143. Krishnan, V.; Lakshmi, T. Bioglass: A Novel Biocompatible Innovation. *J. Adv. Pharm. Technol. Res.* **2013**, *4*, 78–83. [[CrossRef](#)]
144. Fernandes, H.R.; Gaddam, A.; Rebelo, A.; Brazete, D.; Stan, G.E.; Ferreira, J.M.F. Bioactive Glasses and Glass-Ceramics for Healthcare Applications in Bone Regeneration and Tissue Engineering. *Materials* **2018**, *11*, 2530. [[CrossRef](#)]
145. Jones, J.R. Reprint of: Review of Bioactive Glass: From Hench to Hybrids. *Acta Biomater.* **2015**, *23*, S53–S82. [[CrossRef](#)]
146. Sequeira, D.B.; Seabra, C.M.; Palma, P.J.; Cardoso, A.L.; Peça, J.; Santos, J.M. Effects of a New Bioceramic Material on Human Apical Papilla Cells. *J. Funct. Biomater.* **2018**, *9*, 74. [[CrossRef](#)]
147. Morotomi, T.; Washio, A.; Kitamura, C. Current and Future Options for Dental Pulp Therapy. *Jpn. Dent. Sci. Rev.* **2019**, *55*, 5–11. [[CrossRef](#)]
148. Lisa, C.N.; Abraham, S.; Shama Rao, H.N.; Sridhar, N.; Moon, N.; Barde, D.H. A Clinical and Radiographic Evaluation of Periodontal Regenerative Potential of PerioGlas[®]: A Synthetic, Resorbable Material in Treating Periodontal Infrabony Defects. *J. Int. Oral Health* **2014**, *6*, 20–26.
149. Tadjedin, E.S.; de Lange, G.L.; Lyaruu, D.M.; Kuiper, L.; Burger, E.H. High Concentrations of Bioactive Glass Material (BioGranA) vs. Autogenous Bone for Sinus Floor Elevation. *Clin. Oral Impl. Res.* **2002**, *13*, 428–436. [[CrossRef](#)] [[PubMed](#)]

150. Van Vugt, T.A.G.; Geurts, J.A.P.; Blokhuis, T.J. Treatment of Infected Tibial Non-Unions Using a BMAC and S53P4 BAG Combination for Reconstruction of Segmental Bone Defects: A Clinical Case Series. *Injury* **2021**, *52*, S67–S71. [[CrossRef](#)] [[PubMed](#)]
151. Thijssen, E.G.J.; van Gestel, N.A.P.; Bevers, R.; Hofmann, S.; Geurts, J.; van Loo, I.H.M.; Arts, J.J. Assessment of Growth Reduction of Five Clinical Pathogens by Injectable S53P4 Bioactive Glass Material Formulations. *Front. Bioeng. Biotechnol.* **2020**, *8*, 634. [[CrossRef](#)]
152. Greenspan, D.C. NovaMin[®] and Tooth Sensitivity—An Overview. *J. Clin. Dent.* **2010**, *21*, 61–65. [[PubMed](#)]
153. Esteban-Tejeda, L.; Smirnov, A.; Prado, C.; Moya, J.S.; Torrecillas, R.; Bartolomé, J.F. Multifunctional Ceramic-Metal Biocomposites with Zinc Containing Antimicrobial Glass Coatings. *Ceram. Int.* **2016**, *42*, 7023–7029. [[CrossRef](#)]
154. Pazarçeviren, A.E.; Tahmasebifar, A.; Tezcaner, A.; Keskin, D.; Evis, Z. Investigation of Bismuth Doped Bioglass/Graphene Oxide Nanocomposites for Bone Tissue Engineering. *Ceram. Int.* **2018**, *44*, 3791–3799. [[CrossRef](#)]
155. Tripathi, H.; Rath, C.; Kumar, A.S.; Manna, P.P.; Singh, S.P. Structural, Physico-Mechanical and in-Vitro Bioactivity Studies on SiO₂–CaO–P₂O₅–SrO–Al₂O₃ Bioactive Glasses. *Mater. Sci. Eng. C* **2019**, *94*, 279–290. [[CrossRef](#)]
156. Li, Y.; Stone, W.; Schemitsch, E.H.; Zalzal, P.; Papini, M.; Waldman, S.D.; Towler, M.R. Antibacterial and Osteo-Stimulatory Effects of a Borate-Based Glass Series Doped with Strontium Ions. *J. Biomater. Appl.* **2016**, *31*, 674–683. [[CrossRef](#)]
157. Araujo, M.S.; Silva, A.C.; Cabal, B.; Bartolomé, J.F.; Mello-Castanho, S. In Vitro Bioactivity and Antibacterial Capacity of 45S5 Bioglass[®]-Based Compositions Containing Alumina and Strontium. *J. Mater. Res. Technol.* **2021**, *13*, 154–161. [[CrossRef](#)]
158. Leonelli, C.; Lusvardi, G.; Malavasi, G.; Menabue, L.; Tonelli, M. Synthesis and Characterization of Cerium-Doped Glasses and in Vitro Evaluation of Bioactivity. *J. Non-Cryst. Solids* **2003**, *316*, 198–216. [[CrossRef](#)]
159. Saranti, A.; Koutselas, I.; Karakassides, M.A. Bioactive Glasses in the System CaO-B₂O₃-P₂O₅: Preparation, Structural Study and in Vitro Evaluation. *J. Non-Cryst. Solids* **2006**, *352*, 390–398. [[CrossRef](#)]
160. Singh, R.K.; Kothiyal, G.P.; Srinivasan, A. Magnetic and Structural Properties of CaO-SiO₂-P₂O₅-Na₂O-Fe₂O₃ Glass Ceramics. *J. Magn. Magn. Mater.* **2008**, *320*, 1352–1356. [[CrossRef](#)]
161. Kang, X.; Cheng, Z.; Li, C.; Yang, D.; Shang, M.; Ma, P.; Li, G.; Liu, N.; Lin, J. Core-Shell Structured up-Conversion Luminescent and Mesoporous NaYF₄:Yb³⁺/Er³⁺@nSiO₂@mSiO₂ Nanospheres as Carriers for Drug Delivery. *J. Phys. Chem. C* **2011**, *115*, 15801–15811. [[CrossRef](#)]
162. Chatterjee, D.K.; Gnanasammandhan, M.K.; Zhang, Y. Small Upconverting Fluorescent Nanoparticles for Biomedical Applications. *Small* **2010**, *6*, 2781–2795. [[CrossRef](#)] [[PubMed](#)]
163. Li, Q.; Xing, M.; Chen, Z.; Wang, X.; Zhao, C.; Qiu, J.; Yu, J.; Chang, J. Er³⁺/Yb³⁺ Co-Doped Bioactive Glasses with up-Conversion Luminescence Prepared by Containerless Processing. *Ceram. Int.* **2016**, *42*, 13168–13175. [[CrossRef](#)]
164. Kalaivani, S.; Srividiya, S.; Vijayalakshmi, U.; Kannan, S. Bioactivity and Up-Conversion Luminescence Characteristics of Yb³⁺/Tb³⁺ Co-Doped Bioglass System. *Ceram. Int.* **2019**, *45*, 18640–18647. [[CrossRef](#)]
165. Chen, Q.; Zhu, C.; Thouas, G.A. Progress and Challenges in Biomaterials Used for Bone Tissue Engineering: Bioactive Glasses and Elastomeric Composites. *Prog. Biomater.* **2012**, *1*, 1–22. [[CrossRef](#)]
166. Zakaria, S.M.; Sharif Zein, S.H.; Othman, M.R.; Yang, F.; Jansen, J.A. Nanophase Hydroxyapatite as a Biomaterial in Advanced Hard Tissue Engineering: A Review. *Tissue Eng. Part B Rev.* **2013**, *19*, 431–441. [[CrossRef](#)]
167. Oonishi, H.; Hench, L.L.; Wilson, J.; Sugihara, F.; Tsuji, E.; Kushitani, S.; Iwaki, H. Comparative Bone Growth Behavior in Granules of Bioceramic Materials of Various Sizes. *J. Biomed. Mater. Res.* **1999**, *44*, 31–43. [[CrossRef](#)]
168. Khanmohammadi, S.; Ojaghi Ilkhchi, M. Effect of Suspension Medium on the Characteristics of Electrophoretically Deposited Bioactive Glass Coatings on Titanium Substrate. *J. Non-Cryst. Solids* **2019**, *503–504*, 232–242. [[CrossRef](#)]
169. Khanmohammadi, S.; Ojaghi-Ilkhchi, M.; Farrokhi-Rad, M. Evaluation of Bioglass and Hydroxyapatite Based Nanocomposite Coatings Obtained by Electrophoretic Deposition. *Ceram. Int.* **2020**, *46*, 26069–26077. [[CrossRef](#)]
170. Ravarian, R.; Moztarzadeh, F.; Hashjin, M.S.; Rabiee, S.M.; Khoshakhlagh, P.; Tahriri, M. Synthesis, Characterization and Bioactivity Investigation of Bioglass/Hydroxyapatite Composite. *Ceram. Int.* **2010**, *36*, 291–297. [[CrossRef](#)]
171. Rizwan, M.; Hamdi, M.; Basirun, W.J.; Kondoh, K.; Umeda, J. Low Pressure Spark Plasma Sintered Hydroxyapatite and Bioglass[®] Composite Scaffolds for Bone Tissue Repair. *Ceram. Int.* **2018**, *44*, 23052–23062. [[CrossRef](#)]
172. de Siqueira, L.; Grenho, L.; Fernandes, M.H.; Monteiro, F.J.; Trichês, E.S. 45S5 Bioglass-Derived Glass-Ceramic Scaffolds Containing Niobium Obtained by Gelcasting Method. *Mater. Res.* **2021**, *24*, 1–6. [[CrossRef](#)]
173. Hu, S.; Chang, J.; Liu, M.; Ning, C. Study on Antibacterial Effect of 45S5 Bioglass[®]. *J. Mater. Sci. Mater. Med.* **2009**, *20*, 281–286. [[CrossRef](#)]